Science of the Total Environment 1004 (2025) 180693

Contents lists available at ScienceDirect

Science of the Total Environment

journal homepage: www.elsevier.com/locate/scitotenv

Adding invasive alien plant-derived biochar and stinging nettle powder in *Populus nigra* phytoremediation of arsenic- and lead-contaminated Technosol alters microbial community assembly and network stability

Snezhana Mourouzidou [a], Magkdi Mola [a,b], Alex Ceriani [c], Spiros Papakostas [d], Marta Sena-Vélez [e], Efimia M. Papatheodorou [f], Antonio Montagnoli [c], Domenico Morabito [e], Nikolaos Monokrousos [a,*]

[a] University Center of International Programmes of Studies, International Hellenic University, Thessaloniki, 57001, Greece
[b] Soil and Water Resources Institute, Hellenic Agricultural Organization Dimitra, Thermi, Thessaloniki, 57001, Greece
[c] University of Insubria, Department of Biotechnology and Life Science, Via Dunant 3, 21100, Varese, Italy
[d] Department of Science and Technology, School of Science and Technology, University Center of International Programmes of Studies, International Hellenic University, 57001, Thessaloniki, Greece
[e] University of Orléans, P2E-EA1207, INRAE USC1328, Rue de Chartres, Orléans, 45067 Cedex 2, France
[f] Department of Ecology, School of Biology, Aristotle University, Thessaloniki, 54124 Thessaloniki, Greece

HIGHLIGHTS

- Biochar at 5 % reduced microbial diversity and constrained community assembly.
- Fungal communities showed narrower niches and lower resilience than bacteria.
- Co-amendment with nettle and 2 % biochar improved microbial stability.
- Findings support biochar–nettle use in phytoremediation of metal-contaminated soils.

GRAPHICAL ABSTRACT

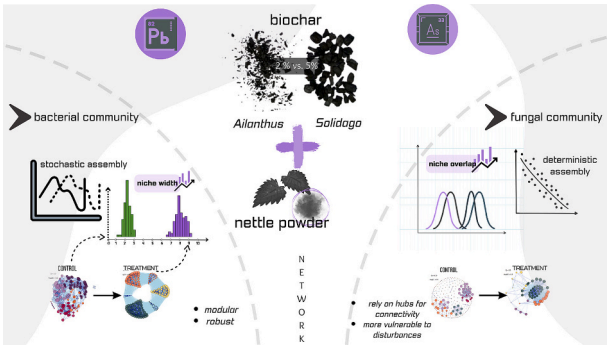

ARTICLE INFO

Keywords:
Biochar
Urtica dioica
Phytoremediation
Heavy metal contamination
Niche adaptation
Network analysis
Microbial community assembly

ABSTRACT

This study examined the effects of biochar and nettle *Urtica dioica* amendments on microbial diversity and community assembly in a historically contaminated Technosol collected from a former silver-lead mine in Pontgibaud (Puy-de-Dôme, France). We investigated how two types of biochar obtained from the biomass pyrolysis of two invasive alien plant species (*Ailanthus altissima* and *Solidago gigantea*) at different doses (2 % vs 5 %), alone and in combination with stinging nettle (*Urtica dioica*) powder inputs that influence the soil's microbial community structure under controlled phytoremediation conditions using *Populus nigra*. We integrated niche theory and network analysis to examine how these amendments alter community-level cohesion and resilience under heavy metal stress, with implications for phytoremediation. We found that a 5 % biochar dose imposed

* Corresponding author.
E-mail address: nmonokrousos@ihu.gr (N. Monokrousos).

https://doi.org/10.1016/j.scitotenv.2025.180693
Received 2 July 2025; Received in revised form 8 September 2025; Accepted 8 October 2025

stronger environmental pressure compared to a 2 % dose, resulting in a significant increase in soil alkalinity and electrical conductivity (EC). In amended soils, bacterial community assembly was primarily driven by stochastic processes, mainly due to dispersal. Fungal communities, in contrast, exhibited reduced stochasticity, particularly under the 5 % biochar–*Solidago* treatments. Furthermore, bacteria expanded their niche width, whereas fungi shifted toward specialist-dominated, narrower niches with greater overlap. The biochar co-application with stinging nettle increased network complexity for both microbial groups; however, the bacterial network responded with higher modularity and more negative links, while the fungal networks were non-modular and exhibited increased positive feedback loops. Network robustness analysis revealed that bacterial networks remained more stable under perturbation across all treatments, whereas fungal networks were more sensitive to hub node loss. Our findings suggest that both the concentration and type of biochar, as well as the presence of *Urtica dioica* amendment, distinctly affect microbial communities and should be carefully considered in designing optimal application regimes and strategies for soil remediation.

1. Introduction

Biochar and other plant-based organic amendments are increasingly used to reclaim degraded areas (Rizwan et al., 2023; Elmeknassi et al., 2024; Aqeel et al., 2023; Mills et al., 2025). For their production, the residual by-products of agriculture—once considered waste—can be repurposed and reintegrated, which reflects the very principles of a circular bioeconomy (Yaashikaa et al., 2020). Supporting circularity and providing a sustainable remediation strategy for contaminated sites, transforming locally abundant biomass derived from the eradication of invasive alien plant species (IAPS), which is also considered waste material to be incinerated, could further enhance IAPS management efforts and reduce their negative impact on ecosystem biodiversity (Ceriani et al., 2025). Biochar, the solid fraction obtained from biomass pyrolysis, is valued for both its physicochemical properties and its ability to immobilize heavy metals due to its high surface area, pore structure, and high adsorption capacity (Mazzurco-Miritana et al., 2025). Additionally, biochar alone may not provide sufficient bioavailable nutrients in heavily polluted soils, and it can be combined with amendments such as compost, mulch, or green manure for enhanced efficiency (Ceriani et al., 2025). One of these is a widely distributed herbaceous perennial plant, *Urtica dioica* L. (known as stinging nettle), which thrives in nutrient-rich and polluted soils (Viotti et al., 2022) and is long recognized as a hyperaccumulator; it can amplify the effects of biochar. Its tissue architecture and compound spectrum mediate metal adsorption (Ertan and Efe, 2019; Bici et al., 2023), and when combined with biochar, simultaneous processes occur at two mechanistic levels: biochar influences metal mobility through sorptive stabilization, whereas *Urtica dioica* residues release organic ligands that chelate heavy metals and facilitate their translocation into the soil solution (Arulselvan et al., 2024). These organic-metal complexes are then readily absorbed by plant roots.

Recent research has well summarized biochar's impact on microbial biomass, diversity, and enzymatic activities (Liu et al., 2022; Zhou et al., 2017; Pokharel et al., 2020; Xu et al., 2023; Deshoux et al., 2023; Adirianto and Bachtiar, 2023; Kerner et al., 2023). A meta-analysis by Deshoux et al. (2023) demonstrated that biochar produced at lower pyrolysis temperatures (350–550 °C) significantly enhanced microbial biomass and diversity, while Liu et al. (2022) found that biochar with lower C/N ratios, particularly those derived from crop residues, had a marked increase in soil microbial carbon biomass. However, the broader questions regarding microbial community stability, resilience, and assembly remain open, especially in the context of contaminated environments. For example, it is known that, in addition to contaminant absorption, biochar can act as a microbial carrier, as reviewed by Bolan et al. (2023). Microorganisms attach to the biochar surface via electrostatic interactions, and subsequently, through multiple adhesion mechanisms (e.g., extracellular polymeric substances), they can grow and spread throughout the carrier surface (Li et al., 2022). This means that biochar's porous structure provides active sites for microbial habitats, especially when in direct contact with a contaminant that causes a loss of microbial activity and diversity (Quilliam et al., 2013; Bolan et al., 2023). By modifying the environmental heterogeneity and resource distribution, biochar can also alter microbial niche dynamics, which can serve as an indicator of community-level stability, particularly under environmental perturbation. For instance, a broader niche (i.e., the spectrum of resources and condition ranges that species can exploit) characterizes generalists, whereas narrower niches are typical of specialists. Specialists dominate stable environments (Muller, 2019), but they also have strong ability to compete across extreme environments (Ren et al., 2023). Generalists are better buffered to environmental stress due to their greater ecological tolerance capacity (Xu et al., 2022), and their proliferation would indicate more resilient microbial communities that can maintain stability across a broader range of environmental conditions/fluctuations, thereby reducing the impacts of disturbances (Xu et al., 2022; Sun et al., 2024a). However, the trade-off is that the replacement of specialist species by generalists eventually leads to functional homogenization (Olden and Rooney, 2006; Clavel et al., 2011; Büchi and Vuilleumier, 2014).

Understanding the assembly processes that govern microbial community composition and structure requires revisiting the seminal idea of Becking (1934), which posits that the environment can act as a strongly selective force at the local scale. When interspecies relationships (e.g., competition, predation, mutualism) or abiotic factors (e.g., pH, salinity, pollution) strongly influence which species persist, the community assembly is considered to be primarily driven by deterministic processes, typically resulting in predictable outcomes. Meanwhile, stochastic processes, as outlined in Hubbell's neutral theory, illustrate how ecological drift and dispersal limitations – including passive displacement - introduce a layer of unpredictability to community assembly. In such settings, a single dominant force is absent, allowing random interactions to shape community structure through probabilistic events (Zhou and Ning, 2017; Bontemps et al., 2024). While it is now widely recognized that both deterministic and stochastic processes co-occur in the assembly of local communities, the discourse continues to center on their relative importance in controlling community structure, succession, and biogeography (Stegen et al., 2015; Zhou and Ning, 2017). For instance, previous studies suggest that plant factors dominate the assembly of microbial communities in non-contaminated environments (Ling et al., 2022; Xiong et al., 2022; Zhong et al., 2022), yet when faced with the added pressures of heavy metals and organic inputs, the patterns of microbial community assembly changes, and is less clear (Xing et al., 2023).

It is not only the composition of the community that determines the system's capacity to maintain structure and function under changing conditions, but also the associations that occur between coexisting members (Gao et al., 2022). In this sense, species co-occurrence networks are very useful indicators, as they present a robust mathematical framework for examining the complexity of relationships within an ecological community (Guseva et al., 2022), and could be valuable in assessing soil restoration outcomes. For example, communities with specific topological characteristics, such as greater modularity and fewer positive associations among taxa, are considered more robust networks (Coyte et al., 2015; Hernandez et al., 2021; Gao et al., 2022).

This is because positive interactions create positive feedback loops between taxa supporting each other's fitness. This, in turn, means that if one member in this loop declines, it has a cascading effect on the others that rely on this interaction (Hernandez et al., 2021). Additionally, modular network architectures are regarded as crucial for the stability and resilience of the entire network. When small-world properties accompany modularity, they confer robustness against random disturbances (Papatheodorou et al., 2021; Stamou et al., 2023). To our knowledge, most phytoremediation studies have relied on conventional organic inputs (e.g., compost, manures) and have assessed outcomes primarily in terms of contaminant immobilization and shifts in taxonomic composition. Our study is the first mesocosm experiment that uses IAPS biomass-derived biochar in combination with stinging nettle powder for the remediation of heavy metal-contaminated technosols. It also integrates a more comprehensive ecological framework, such as null modeling, niche breadth and overlap, and network analyses, which are rarely applied in phytoremediation studies. Given the growing evidence suggesting that biochar does not always have favorable effects on soil and soil biota, and that its impact on specific microorganisms cannot be generalized (Brtnicky et al., 2021), the limited research on nettle-based amendments further compounds this. Hence, it is necessary to identify thresholds or optimal application regimes for more effective phytoremediation and restoration practices.

Our specific objectives were to: (1) determine the type and dose of biochar and/or amendment combinations that impact microbial community structure and assembly processes the most; knowing that under contamination, communities tend to be dominated by deterministic assembly as evidenced by Zhang et al. (2022), Jiang et al. (2021) and Liu et al. (2023), we nevertheless anticipate the addition of amendments to change this pattern, most likely in a dose-dependent manner; (2) examine how labile and recalcitrant amendments differentially influence niche breadth within bacterial and fungal communities, according to their substrate-use capacities and ecological strategies. This builds on the understanding that substrate characteristics shape microbial resource use (Wang and Kuzyakov, 2024). Bacteria, which typically prevail in environments with readily available, labile carbon sources (such as those in nettle) due to their higher growth rates, efficient uptake, and small cell size, would likely expand their niche in the nettle-amended soil. When the substrate is composed of recalcitrant, hydrophobic compounds like those found in biochar, it is most likely that fungi would dominate as they produce broad-spectrum exoenzymes and exploit spatial niches via hyphal foraging, and therefore, in biochar-amended soils alone, fungal communities may increase their niche width; (3) determine the conditions under which microbial co-occurrence networks show greater resilience and/or robustness, and which settings make them more vulnerable to disturbance. For example, Zhu et al. (2022) found that the node-level topological characteristics of the subcommunities were more complex under biochar treatment, with differences based on the type of biochar used for soil remediation. Therefore, we aim to assess how combinations of amendments and their corresponding doses influence the robustness and structural features of microbial networks, including modularity, robustness, and the presence of keystone taxa.

2. Materials and methods

2.1. Soil and amendments

The contaminated soil (Technosol) was sampled from a former silver-lead mine in Pontgibaud (Puy-de-Dôme, France; 45.8331° N, 2.8511° E). The topsoil (0–20 cm) was sampled with a steel shovel and transferred into polyethylene bags. For each treatment, five replicate pots were prepared, and all analyses were performed on these biological replicates. The soil was air-dried. Values such as pH and electrical conductivity (EC), were determined using a pH-EC meter (Seven Excellence, Mettler-Toledo AG, Switzerland). Pseudo-total Arsenic (As) and Lead (Pb) concentrations were determined via ICP-AES (ULTIMA 2, HORIBA, Labcompare, San Francisco, USA). Specifically, 0.2 g of soil was mixed with a 1:3 (v/v) solution of 65 % HNO3 and 37 % HCl. Samples were digested using a pressurized vacuum microwave system (Multiwave 3000, Anton Paar GmbH, Austria). They were then collected in a 50 mL flask, brought up to 25 mL with ultra-pure water, and filtered through a 0.45-μm nitrocellulose membrane for the ICP-AES measurements.

Biomasses of *Ailanthus altissima* and *Solidago gigantea* were collected in Lombardy (northern Italy), chipped (~7 cm^2; GeoTech PCS70L), dried for two weeks at 25 °C, and milled through a 4 mm sieve (mill Retsch SM 300). Biochar was prepared through slow pyrolysis at 550 °C with a residence time of 45 min (heating rate of 20 °C min^{-1}) under a nitrogen flow (*Re*-Cord, Scarperia e San Piero, Italy). Commercial powdered stinging nettle (*Urtica dioica*) (Orties broyées Algoflash Naturasol, France) was used as the other amendment. Biochar and stinging nettle's pH and EC were measured (see above). The carbon, hydrogen, and nitrogen (CHN) content was determined for all amendments (*Ailanthus biochar*, *Solidago biochar*, and *Urtica dioica* powder) and the bulk soil using a FlashEA 1112 series CHNS analyzer (Thermo Scientific). Full results are provided in Supplementary Table S1.

2.2. Experimental design

The growing medium was prepared in different weight proportions to a final mass of 550 g. In total, ten different treatments with five replicates each were prepared (n = 50): a control composed of Pontgibaud (PG) soil alone. Two treatments included biochar derived from *Ailanthus* at concentrations of 2 % (BA2) and 5 % (BA5), while two others included biochar from *Solidago*, also at 2 % (BS2) and 5 % (BS5). One treatment consisted of PG mixed with 2 % powdered stinging nettle alone (O). The remaining four treatments combined nettle with biochar: PG with 2 % nettle and 2 % *Ailanthus* biochar (OBA2), 2 % nettle and 5 % *Ailanthus* biochar (OBA5), 2 % nettle and 2 % *Solidago* biochar (OBS2), and 2 % nettle and 5 % *Solidago* biochar (OBS5). The amendment rates of 2 % and 5 % (w/w) were selected based on a pilot study (Ceriani et al., 2025), as well as on previous studies demonstrating significant effects on soil pH, As and Pb immobilization, and microbial community shifts in contaminated Technosols (e.g., Lebrun et al., 2017; Lomaglio et al., 2018; Palmeggiani et al., 2021).

The mixtures were left to stabilize for four weeks before *Populus nigra* cuttings were directly added to the mixtures. The plants were grown for 47 days in a culture chamber (20 ± 5 °C), with 800 μmol m^{-2} s^{-1} light intensity and a 16/8-hour light/dark photoperiod. Pots were randomly distributed across trays within the growth chamber and periodically repositioned to minimize positional bias. Soil moisture was maintained at field capacity through daily irrigation with tap water.

2.3. Microbial analysis

Microbial DNA was extracted on day 47 of the experiment using the NZY Microbial gDNA Isolation Kit (USA) following the manufacturer's protocol. We selected this time point because it reflects a stabilized microbial state after the initial fluctuations following amendment addition. DNA concentration was measured using a Q3000 UV spectrophotometer (Quawell Technology, San Jose, USA). The full-length bacterial 16S rRNA gene was amplified using primers 27F and 1492R, while the fungal ITS2 region was amplified with ITS86F and ITS4 primers. PCR conditions included an initial denaturation at 95 °C for 3 min, followed by 30 cycles (98 °C for 20 s, 61 °C for 15 s for bacteria or 60 °C for fungi, and 72 °C for 1 min), and a final extension at 72 °C for 2 min. PCR products were stained with Xpert Green DNA Stain (QRiSP, Portugal) and visualized on a 1.0 % agarose gel to confirm integrity. Sequencing was performed using the MinION platform (Oxford Nanopore Technologies, UK) with R10.4 flow cells, following the manufacturer's standard protocols. Base-calling, demultiplexing, and barcode

trimming were performed using Guppy v3.2.10. Amplicon sequence variants (ASVs) were inferred using DADA2 (v1.26.0). Taxonomic classification was performed using the SILVA SSU v138.1 database for bacteria and the UNITE database for fungi. Non-target ASVs (e.g., chloroplasts, mitochondria) and singletons/doubletons were removed, resulting in 258 fungal and 446 bacterial taxa. Samples with low sequencing depth were excluded, and those with >50 % missing or zero values across taxa were removed. After filtering and read normalization based on median depth, the final dataset included 92 fungal and 234 bacterial taxa. All sequence data have been submitted to the NCBI Sequence Read Archive, accessible through the accession number PRJNA1273486.

2.4. Statistical analysis

All statistical analyses were conducted using RStudio (version 4.4.1). Alpha diversity metrics were calculated using the *phyloseq* package (McMurdie and Holmes, 2013). Bray-Curtis distances based on the relative abundance of microbial communities were computed to assess dissimilarities between treatments using non-metric multidimensional scaling (NMDS; Kruskal, 1964) and analysis of similarity (ANOSIM; Clarke, 1993). The differential abundance of microbial taxa was analyzed using the LEfSe (Linear Discriminant Analysis Effect Size) method, as implemented in the *microeco* package (Liu et al., 2021). *p*-Values were adjusted for multiple comparisons using the Benjamini-Hochberg (BH) method (Benjamini and Hochberg, 1995). The LDA score threshold was set to 4.0. Niche breadth and niche overlap were quantified using Levin's index (Levins, 1968) to assess, respectively, the degree of ecological generalism within microbial communities and the extent of resource or habitat use similarity among taxa. A broader niche indicates a more generalist ecological strategy, while a narrower niche reflects specialization. Niche overlap refers to the extent to which two species share the same carbon source in their metabolic processes (Ji and Wilson, 2002), with a greater overlap indicating increased metabolic similarity. Both metrics were implemented using the *spaa* package (Zhang, 2016).

2.4.1. Null modeling and community assembly mechanisms

To assess whether observed β-diversity patterns deviated from random expectations, we applied a null model approach following Tucker et al. (2016), using the 'oecosimu' function with the 'swap' algorithm. The Sørensen dissimilarity was used as the target metric, and 999 randomizations were performed. As neither bacterial nor fungal communities showed significant deviations from null expectations (SES $\approx$ 2.06 and 0.21, respectively; $p > 0.05$) (Table S2), we proceeded to quantify the balance between stochastic and deterministic processes. We further applied a null modeling-based approach similar to that of Ning et al. (2019); we calculated the Normalized Stochasticity Ratio (NST) using treatment-level pooled data for both bacterial and fungal communities, which compares the observed community structure to that generated by a null model. The boundary for distinguishing between deterministic (<50 %) and stochastic (>50 %) assembly was set at a normalized stochasticity ratio of 50 % (Li et al., 2022). To further confirm the contribution of neutral processes to microbial community assembly, we applied the Sloan neutral community model (Sloan et al., 2006). The model fits observed frequencies against predicted probabilities under a beta distribution, parameterized by the average community size (mean total OTUs per sample, *N*) and the migration rate (*m*), which reflects the probability that an OTU absent from a local community is replaced by immigration from the metacommunity. The detection limit (*d*) was set as 1/mean(*N*). Model fitting was performed in R using the 'mle2' function from the *bbmle* package (Nelder-Mead method), which maximizes the log-likelihood of the residuals between observed and expected OTU frequencies. The goodness of fit to the neutral model was assessed using R^2 as the coefficient of determination.

2.4.2. Co-occurrence network and network stability

Before network construction, the data underwent a filtering process to retain only ecologically meaningful taxa. We ensured that individual taxa were present in at least three out of five replicates of each experimental group so that network links were based on consistently present organisms rather than sporadic detections. Taxa with zero variance across samples were removed, as their invariant abundance cannot contribute to the correlation structure. This procedure reduces noise from rare or unstable taxa. A Spearman correlation matrix was constructed using the *igraph* package, with a correlation threshold of $|r| > 0.7$ and with *p*-values adjusted for multiple testing using the Benjamini-Hochberg (BH) procedure to retain robust associations. There has been considerable criticism of relying solely on network metrics, such as betweenness or degree centrality, as multiple confounding factors can influence these. To address this limitation, we employed a perturbation-based approach, which is in line with recommendations from Valiente-Banuet et al. (2019), Karimi et al. (2017), and Guseva et al. (2022), who suggested testing network models and ecosystem resilience through a perturbation approach (e.g., node or edge removal), rather than relying on correlative patterns alone. The simulation framework comprised two removal scenarios designed to evaluate network robustness under species loss. Random removal mimics diffuse stochastic extinctions driven by chance demographic drift or small-scale environmental fluctuations, whereas targeted removal approximates selective pressures that can disproportionately eliminate hub taxa and thereby destabilize network connectivity (Dunne et al., 2002). The first scenario implemented random node removal (i), in which 20 % of nodes were eliminated to simulate stochastic species loss events common in natural systems. The second scenario applied targeted removal (ii), wherein the top 5 nodes with the highest betweenness centrality were selectively removed. Betweenness centrality identifies key nodes that serve as bridges or connectors within the network, and their removal allows us to test the resilience of the network to the loss of highly influential species. Additionally, we quantified the impact of node removal on two stability metrics—the size of the Largest Connected Component (LCC) and Natural Connectivity (NC), following approaches recommended for evaluating structural resilience (Jun et al., 2010; Jiang et al., 2024), where LCC reflects network fragmentation and NC captures overall connectivity redundancy and robustness. The effects of these perturbations on network stability metrics were statistically assessed using analysis of variance (ANOVA) on the resulting model outputs. To evaluate the resilience of microbial co-occurrence networks to random disturbances, we applied a robustness metric based on random graph theory (Liu et al., 2017). We calculated the *p_rc* index, which estimates the critical fraction of nodes that must be removed before the network fragments. It is defined as:

$$p_c{}^r = 1 - \frac{1}{\mathrm{Ko} - 1}$$

where K_0 is the ratio of the average squared degree (K_2) to the average degree (K), expressed as $K_0 = K_2/K$. Higher values of *prc* indicate a more robust network, whereas negative values suggest that the network is prone to disintegration in case of random node loss. This metric assesses the network's resilience to disruptions.

To identify the determinants of microbial network stability, we implemented Random Forest (RF) models using the *caret* R package (Kuhn, 2008). This approach allowed us to test whether network stability was shaped more by the internal architecture of the community (e.g., the presence of hub taxa or node centrality) or by the external amendment treatments. The response variable was the stability impact, calculated as the proportional reduction in the most significant connected component following the removal of an individual node, thus reflecting the structural contribution of each taxon to network robustness. Predictor variables included five node-level topological metrics—degree, betweenness, closeness, eigenvector centrality, and hub

score—as well as treatment identity, a categorical factor representing environmental conditions. This yielded a dataset of 1036 fungal nodes and 1857 bacterial nodes — each representing an individual taxon under a specific treatment condition, each analyzed separately, with the same six predictor variables. RF models were trained using 10-fold cross-validation, and hyperparameter tuning was performed over a range of entry values to optimize performance based on Root Mean Square Error (RMSE). To assess the contribution of individual features to model predictions, we extracted variable importance scores using the varImp() function. This approach estimates the impact of each predictor on overall model accuracy by quantifying changes in prediction error after 999 permutations, allowing inference about the relative ecological significance of network attributes and treatments in shaping node stability.

2.4.3. Environmental variables

Among the environmental variables considered were arsenic (As), lead (Pb), electrical conductivity (EC), pH, and the bioconcentration factor (BCF). The BCF was calculated as the ratio of the metal concentration in plant roots (mg kg^{-1} dry weight) to the corresponding metal concentration in soil (mg L^{-1} or mg kg^{-1}) for each treatment. BCF values were normalized to enable comparison across treatments. To determine predictors of changes in microbial diversity and niche width, we applied structural equation modeling (SEM) using the *lavaan* and *semPlot* packages in R (Rosseel, 2012; Epskamp, 2015). Standard errors and confidence intervals were estimated via bootstrapping (1000 iterations) to account for sampling variability and potential deviations from normality. Redundancy Analysis (RDA) was performed using *vegan* package (Oksanen et al., 2022), and significance was assessed using 999 permutations (Legendre and Legendre, 2012). Spearman rank correlation (Spearman, 1904) was calculated between the environmental variables and bacterial and fungal taxa.

3. Results

3.1. Soil physicochemical properties

In the untreated control, the pH remained distinctly acidic—a condition under which metalloids, such as As, are often immobilized within the soil matrix. The introduction of amendments initiated a substantial shift, with all treatments experiencing a significant increase in pH, particularly in OBA5 and OBS5, where the strongest alkaline transitions were observed (Fig. 1; Table 1). Electrical conductivity increased similarly across treatments, particularly in those enriched with *Solidago*-derived biochar (OBS2, OBS5), following a concentration-dependent

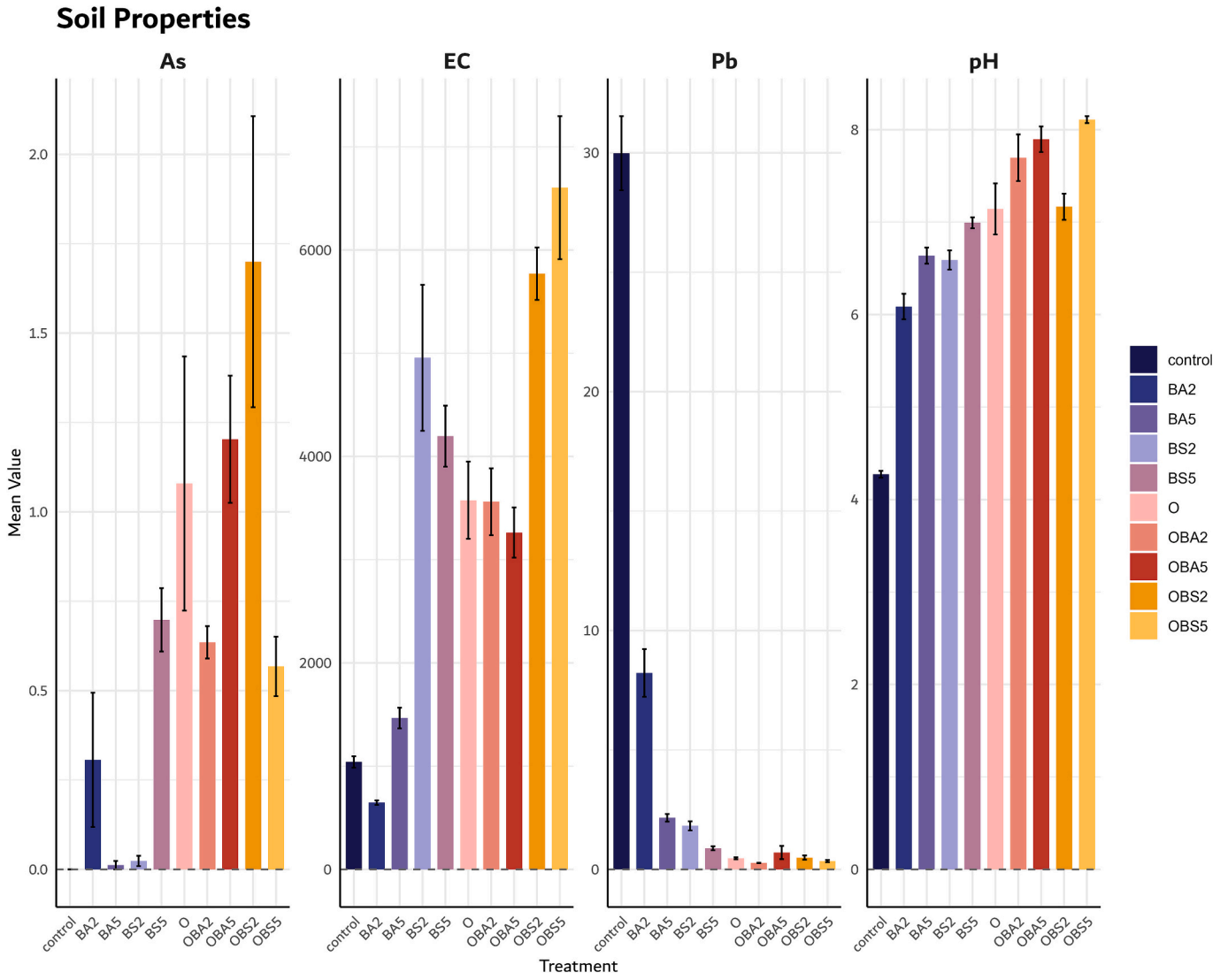

Fig. 1. Changes in soil physico-chemical properties: Arsenic (As) (mg kg^{-1}), Lead (Pb) (mg kg^{-1}), Electrical conductivity (EC) (μS cm^{-1}), and pH, across non-amended soil (control) and different treatments (mean ± SE).

Table 1
Soil properties across different treatments. Results are presented as mean ± SD. Significant differences ($p < 0.05$) among treatments are indicated by lowercase letters, detected by Duncan's multiple range test.

Treatment	pH	EC	As	Pb
Control	4.27 ± 0.08e	1040.62 ± 124e	0e	29.98 ± 3.4a
BA2	6.09 ± 0.3d	646.52 ± 49.7e	0.77 ± 0.42de	8.22 ± 2.2b
BA5	6.64 ± 0.1c	1466.42 ± 224e	0.06 ± 0.02e	2.16 ± 0.3c
BS2	6.59 ± 0.2c	2258.3 ± 158bc	0.020 ± 0.03e	1.82 ± 0.4c
BS5	6.99 ± 0.1bc	4196.7 ± 662cd	0.7 ± 0.19bcd	0.88 ± 0.1c
O	7.14 ± 0.6c	3576.38 ± 836d	1.08 ± 0.7bc	0.46 ± 0.09c
OBA2	7.56 ± 0.5a	3061.07 ± 723d	0.64 ± 0.1bcde	0.26 ± 0.02c
OBA5	7.73 ± 0.3a	3196.68 ± 544d	1.14 ± 0.3bab	0.76 ± 0.60c
OBS2	7.22 ± 0.3b	5630.62 ± 155ab	1.63 ± 0.9a	0.4 ± 0.1c
OBS5	8.11 ± 0.08a	6617.25 ± 58.3a	0.51 ± 0.1cde	0.45 ± 0.1c

pattern, where 5 % applications were consistently higher than those at 2 % treatments. Mediated by pH, arsenic, previously bound under acidic conditions, was released into bioavailable forms, with the highest As concentration recorded in OBA5 and OBS2. By contrast, Pb levels in the control group were 29.98 ± 2 mg kg^{-1} and significantly declined in response to the treatments, with the lowest value recorded in OBA2 and OBS2.

3.2. Microbial diversity and composition

The response of microbial diversity to treatments demonstrated significant changes in bacterial, but not fungal, diversity across sampling areas (Fig. 2; Table S3). Bacterial richness metrics (i.e., Chao1 and Observed indices) remained constant across treatments. However, Shannon-Weiner and Simpson indices were significantly different across some treatments. An increase in Shannon-Weiner diversity was observed in the combination treatments OBA2, OBS2, and OBS5 compared to the control ($F = 7.8$, $p < 0.05$). The lowest diversity was recorded in BA5 and BS5. For the Simpson index, only the OBS2 treatment showed significant difference compared to the control ($F = 2.2$, $p < 0.05$). The InvSimpson index, a measure of community evenness, similarly demonstrated higher diversity in both OBA2 and OBS2 compared to the control and the 5 % biochar treatments ($F = 9.8$, $p < 0.05$).

Stacked bar charts (Fig. 2) show that Cyanobacteria and Bacillota were dominant in the control, but their relative abundance decreased in the OBA2, OBA5, OBS2, and OBS5 treatments. In these treatments, Bacteroidota and Dependentiae increased in abundance. Kruskal-Wallis tests indicated significant differences in multiple phyla across treatments, including Acidobacteriota, Armatimonadota, Candidatus Eremiobacterota ($p < 0.001$), and Bacillota and Bacteroidota ($p < 0.05$). For fungal communities, the family Coniochaetaceae was the dominant taxon in the control and showed a marked decrease in abundance in the BS2 treatment (Fig. 3). LEfSe analysis identified Cyanobacteria as a biomarker for the control, while *Paracremonium* and Zopfiella were the only fungal genera with significant abundance differences among treatments (Fig. S1; Fig. S2).

To compare the structure of microbial communities, non-metric multidimensional scaling (NMDS) analyses were conducted for bacteria and fungi (Fig. 3). ANOSIM analysis of bacterial community structure revealed a strong separation between treatment groups ($R = 0.8$, $p < 0.001$) (Fig. 2). The only non-significant pairwise comparison was observed between the OBA2 and OBA5 groups. For fungal communities, ANOSIM indicated a weaker but statistically significant separation ($R = 0.13$, $p = 0.01$). Significant differences were identified between the following treatment pairs: control vs. OBS5, control vs. BS2, and BA2 vs. OBS5.

3.3. Microbial community assembly

3.3.1. Niche width and overlap

Niche breadth was calculated using Levins' index, which quantifies the distribution of each taxon's abundance across samples within a treatment group (Table 2). The widest niches were observed in the treatments OBA2 and OBS2 (biochar 2 %) and the narrowest in OBA5 for the bacterial group. For fungi, the control, O, OBA2, and OBA5 (*Ailanthus*-derived biochar) had the widest niches, while the smallest values were observed for BA2, OBS2, and OBS5 (*Solidago*-derived biochar). The niche overlap values between bacterial taxa across different treatments ranged from 0.51 to 0.89, with significant treatment-specific variations ($p < 0.001$). The highest mean overlap was observed in the BA2 and OBA2 (*Ailanthus*-derived biochar at 2 %) treatments, and the lowest mean overlap occurred in the stinging nettle-amended soil (O). For fungal species, the lowest niche overlap was observed in the control and the highest in BA2. These observations suggest an overall pattern where niche overlap is inversely correlated with niche breadth.

3.3.2. Processes that dominate microbial community assembly

The Normalized Stochasticity Ratio (NST) based on the Jaccard distance index (absence-presence data) showed that stochastic processes dominated bacterial assembly (50–78 %), in contrast to fungal communities (22–45 % stochasticity) (Table S4). The treatment under the highest environmental selection was BA2 for bacteria and OBS5 for fungi. To further dissect the role of dispersal-driven stochasticity, we applied the Sloan neutral model (Fig. 4), in which the estimated migration rate (m) represents the probability that a random loss (death or immigration) of an OTU in a local community is replaced by immigration from the metacommunity. Higher m values suggest a stronger influence of dispersal, while lower m values reflect limited connectivity or stronger environmental filtering.

Bacterial communities exhibited higher m values in the control and in the treatment with *Ailanthus*-derived biochar ($m = 1.28$, 1, and 0.87, respectively), consistent with a strong dispersal influence. In contrast, co-amended soils with 5 % biochar showed a reduced m value and, therefore, a reduced dispersal rate (OBA5: $m = 0.2$, OBS5: $m = 0.03$). This means that other stochastic forces (e.g., ecological drift or priority effects) played a role in shaping community assembly. Fungi remained deterministic except in the BA2/BA5 (Table 3; Fig. 4). In treatments with *Solidago*-derived biochar, such as BS2 ($m = 0.04$), OBS2 ($m = 0.02$), and OBS5 ($m = 0.03$), there was a strongly reduced level of immigration, whereas treatments O and OBA5 showed comparatively higher m rates ($m = 0.4$ and 0.3, respectively), implying a loosening of dispersal limitation.

3.4. Network community structure

3.4.1. Bacterial networks

Ten molecular ecological networks were constructed using the microbial sequencing results of soils treated with different types and concentrations of biochar and stinging nettle powder. The correlation coefficient threshold for these networks was determined to be >0.7. The number of bacterial ASVs used for network construction was, on average, 26.5 % greater in the control than under the experimental conditions, specifically BA2 (21.69 %), BA5 (21.48 %), BS2 (9.8 %), and BS5 (25.96 %). Treatments like OBA2, OBA5, OBS2, and OBS5 also showed lower ASV presence, ranging from 11.76 % to 29.79 % across replicates. The total number of links and nodes in the BS2 network was higher than that in the control; however, all treatments containing stinging nettle powder, despite having fewer nodes than the control, exhibited a surge in link density, with an apparent increase in AvgK and AvgCC (Table S5).

The number of negatively correlated links in the BA2 and BA5 networks was 1246 and 1413, respectively, accounting for 39.07 % and 38.68 % of the total number of corresponding links; the number of

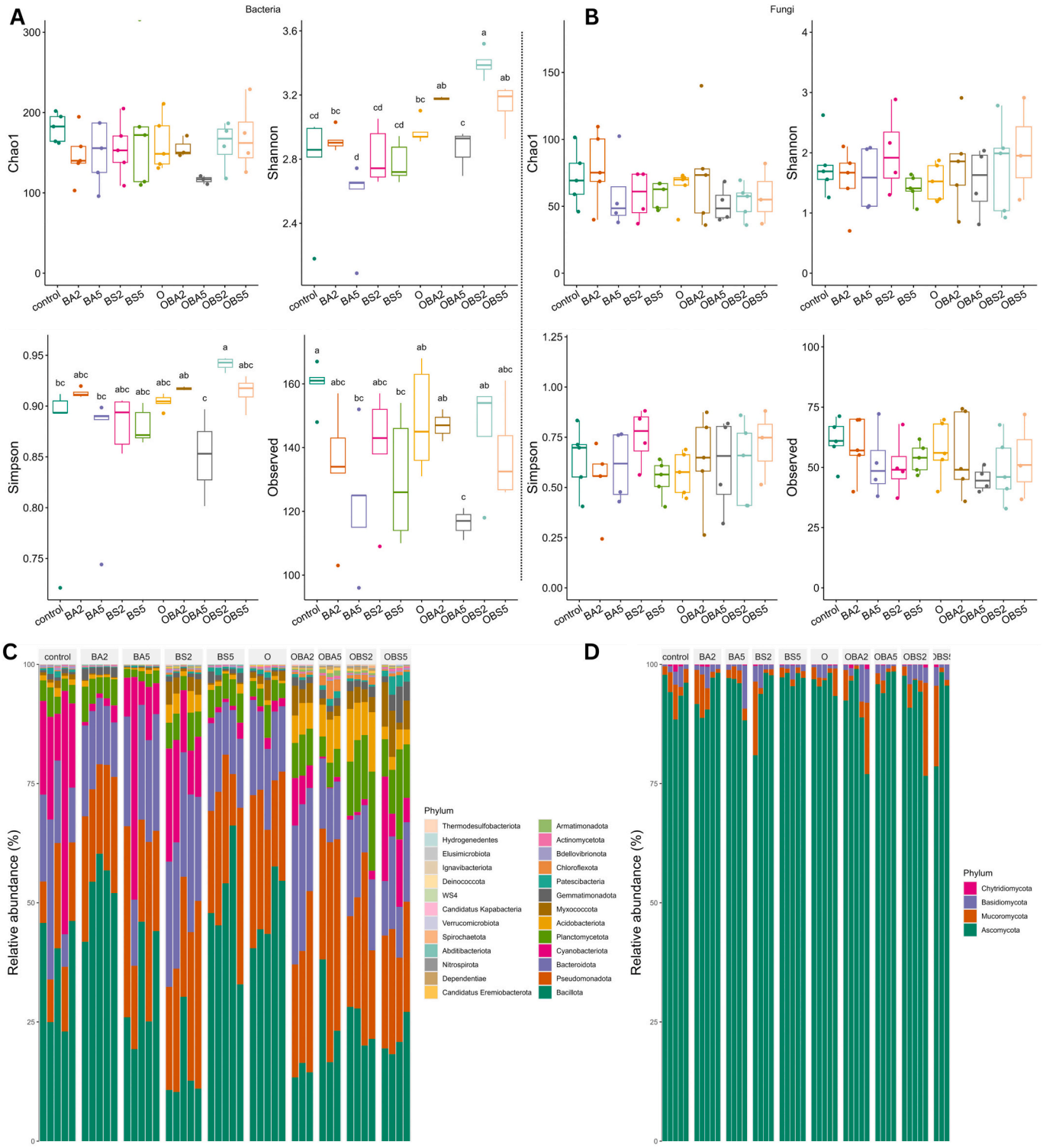

Fig. 2. Box plots depicting the distribution of alpha diversity indices across different treatments for soil bacteria (A) and fungi (B). The central line of each box represents the median, with the box indicating the interquartile range and whiskers extending to the minimum and maximum values. The below plot depicts the composition of microbial phyla, represented by different color shades within each phylum, for soil bacteria (C) and fungi (D) in terms of relative abundance across treatments.

negatively correlated links in the BS2 and BS5 networks was 2445 and 1760, respectively, accounting for 46.14 % and 46.33 % of the total number of corresponding links. Notably, the highest percentage of negative correlations was observed in the OBA2 network, at 47.8 %, while the lowest percentage was found in the control network, at 32.4 %. In addition, the average modularity in BA2, BA5, BS5, O, OBA2, and OBA5 was higher than that in the control. The control network exhibited the highest centralization (0.6), while the lowest centralization values were observed in OBA2, OBA5, and OBS5 (Fig. 5).

3.4.2. *Fungal networks*

The number of fungal ASVs used for network construction remained

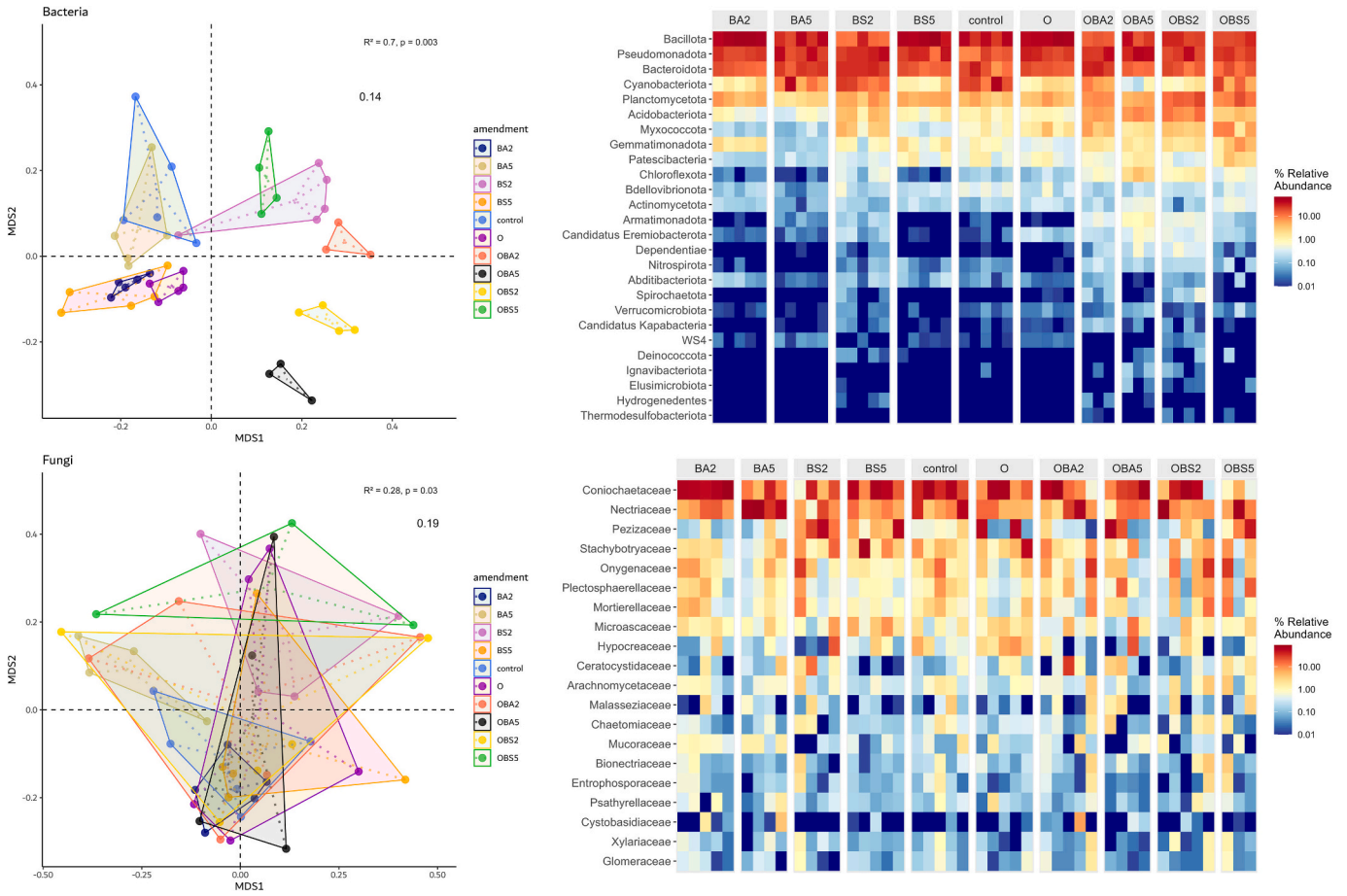

Fig. 3. Nonmetric multidimensional scaling (NMDS) based on Bray–Curtis distance matrix was used to visualize microbial composition at the genus level. Polygons enclose 95 % of the data for each group. Different colors represent different amendment treatments. More overlap indicates a higher degree of similarity between treatments. Heatmaps, based on the respective NMDS ordination illustrates the abundance of the most abundant taxa at the Family level across the 10 treatments.

Table 2
Summary statistics (mean, range, ±SD) of niche width and niche overlap for each treatment, with statistical results from ANOVA indicating significant differences (F-values and *p*-values) between treatments.

Treatment	Niche width		Niche overlap	
	Bacteria	Fungi	Bacteria	Fungi
	Mean(±sd)		Mean(±sd)	
Control	8.84 ± 3.05cde	2.41 ± 0.1.1ab	0.62 ± 0.34cde	0.43 ± 0.39f
BA2	11.5 ± 0.5bc	1.33 ± 0.5bc	0.89 ± 0.25bc	1.05 ± 0.14a
BA5	8.16 ± 2.4de	1.7 ± 0.5de	0.61 ± 0.33de	0.67 ± 0.36d
BS2	8.9 ± 1.7cde	2.09 ± 0.5e	0.65 ± 0.32cde	0.63 ± 0.4bde
BS5	8.5 ± 1.3de	2.12 ± 0.55a	0.76 ± 0.24de	0.69 ± 0.15d
O	10.5 ± 0.7bcd	2.42 ± 0.53ab	0.51 ± 0.34bcd	0.59 ± 0.15e
OBA2	12.1 ± 0.2 b	2.32 ± 0.49de	0.74 ± 0.3b	0.68 ± 0.13b
OBA5	7.18 ± 2.3b	2.2 ± 0.5 cd	0.62 ± 0.23e	0.69 ± 0.34d
OBS2	17.2 ± 1.8a	1.29 ± 0.5de	0.61 ± 0.37a	0.88 ± 0.13c
OBS5	11.9 ± 2.07 b	1.92 ± 0.43f	0.55 ± 0.3b	0.66 ± 0.27d
F	9.8, $p <$ 0.000.1***	12.8, $p <$ 0.001**	66.7, $p <$ 0.001***	68.86, $p <$ 0.0001***

relatively consistent across most treatments. Treatments OBA2, O, and BA2 showed greater ASVs compared to the control. The lowest ASV presence was observed in OBA5 (17.5 % lower than in the control), followed by BS5 (5.9 % lower) and OBS5 (4.7 % lower). The total number of links and nodes in the BA2 and OBA2 networks were higher than those in the control, with the lowest values observed in BS5, OBS5, and OBA5 (Table S6).

The average degree (Avgk), representing the average number of connections per node, was highest in the O treatment (19.8) and lowest in the OBA5 and OBS5 treatments (15.1 and 17.9, respectively) (Table S6). All treatments showed similar average clustering coefficients (AvgCC) of approximately 0.5, indicating moderately clustered networks. The average path length across treatments ranged from 1.5 to 1.7. The Small-Worldness Index for all fungal networks exceeded 1, ranging from 2.4 to 2.74. The modularity values for fungal networks varied between treatments but were generally below 0.4, indicating a non-modular structure in fungal networks, which in turn suggests a relatively homogeneous interaction structure without clear partitioning into distinct modules (Fig. 6). The number of negative edges was low across all treatments.

To validate the non-random architecture of the microbial co-occurrence networks, we compared each observed bacterial and fungal network against 100 Erdős–Rényi (ER) random networks of equivalent size and edge density. Observed networks consistently exhibited higher modularity (Q = 0.32–0.79 vs. ER: Q = 0.06–0.45), elevated clustering coefficients (C = 0.52–0.94 vs. ER: C = 0.01–0.38), and comparable or shorter average path lengths (L = 0.25–1.85 vs. ER: L = 1.06–4.90) than their corresponding Erdös–Réyni random network,

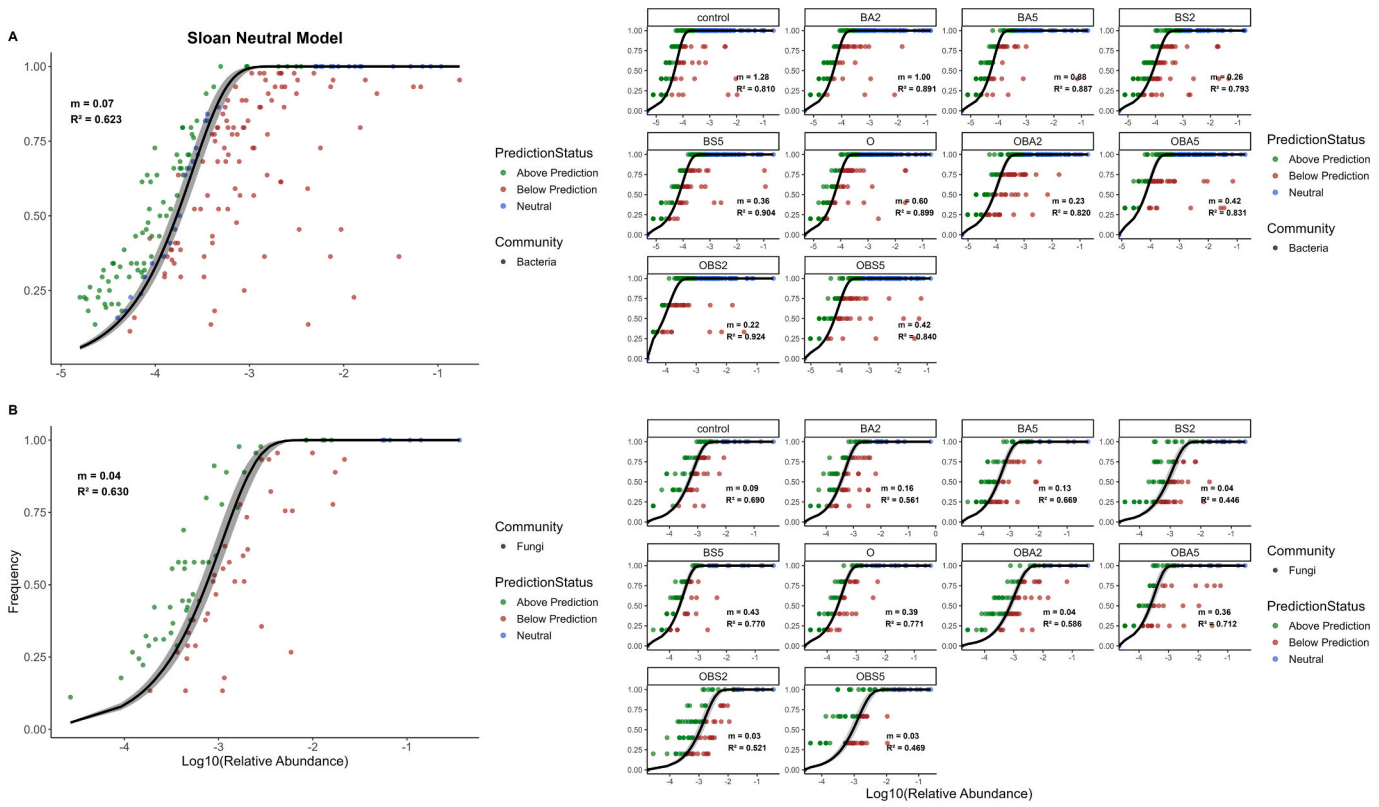

Fig. 4. The plot compares observed and predicted OTU occurrence frequencies for bacteria (A) and fungi (B) across treatments. Points show the observed frequency (y-axis) vs. log-transformed mean relative abundance (x-axis), colored by prediction status: green for "Above Prediction," grey for "On Prediction," and red for "Below Prediction." The black line denotes the predicted occurrence frequency, with the surrounding grey shading indicating the 95 % CIs. R^2 values and migration probabilities (m) for each group are also shown.

Table 3
Application of Sloan's neutral model to bacterial and fungal communities across treatments. The table presents the estimated immigration probability (m), model fit (R^2), total species richness, sigma (σ^2) as a measure of deviation from neutrality, and the proportion of species classified as below neutral (negatively selected), neutral (stochastic), or above neutral (positively selected).

Group	m		R^2		Total taxa		Below neutral		Neutral		Above neutral	
Fungi	0.04		0.63239		92		42.4		6.52		51.1	
Bacteria	0.07		0.62292		234		46.6		5.98		47.4	
	Bacteria	Fungi	b	f	σ^2 bac	σ^2 fungi	b	f	b	f	b	f
Control	1.27	0.08	0.8	0.68	0.18	0.2	12.82	33.69	40.17	43.47	47.01	22.82
BA2	1	0.16	0.89	0.56	0.14	0.23	13.25	38.04	44.87	42.39	41.88	19.56
BA5	0.87	0.13	0.88	0.66	0.15	0.21	10.68	28.26	38.89	53.26	50.43	18.47
BS2	0.25	0.04	0.79	0.44	0.18	0.27	24.79	36.95	25.21	43.47	50	19.56
BS5	0.36	0.43	0.9	0.76	0.13	0.18	18.8	20.65	37.18	51.08	44.02	28.26
O	0.6	0.39	0.89	0.77	0.13	0.17	18.38	26.08	39.74	52.17	41.88	21.73
OBA2	0.42	0.04	0.83	0.58	0.17	0.22	15.81	40.21	41.88	45.65	42.31	14.13
OBA5	0.22	0.35	0.92	0.71	0.12	0.22	11.11	28.26	52.56	38.04	36.32	33.69
OBS2	0.42	0.02	0.84	0.52	0.17	0.25	18.8	33.69	43.16	50	38.03	16.3
OBS5	0.22	0.03	0.81	0.46	0.18	0.27	22.22	33.7	35.47	41.3	42.31	25

revealing that microorganisms in all the compartments assembled nonrandomly.

3.4.3. *Keystone taxa and topological features in microbial network stability*

Typically, nodes with Pi >0.62 or Zi > 2.5 are classified as keystone taxa (Deng et al., 2012). Keystone taxa, which are integral both within their respective modules and across modules, are often located in network hubs, module hubs, or serve as connectors (Fig. 7). Overall, the bacterial phyla Bacteroidota and Planctomycetota were consistently prevalent as keystone taxa across all plots. In the fungal networks, most connectors and the only module hub belonged to the phylum Ascomycota (Table S7).

For both fungal and bacterial datasets, the RF models demonstrated high predictive power (fungi: $R^2 = 0.9$, RMSE = 0.01; bacteria: $R^2 = 0.9$, RMSE = 0.0005). In fungal communities, node centrality metrics, such as closeness and betweenness, showed a moderate influence, but treatment identity emerged as the dominant predictor. Unlike in fungi, in bacterial communities, closeness centrality was a stronger predictor of node-level stability, suggesting that resilience depends on how efficiently information spreads across the network.

Bacterial networks consistently demonstrated high stability across all treatments, with minimal variation in response to random disturbances. In contrast, fungal networks showed much lower and more variable stability values under the same scenario, ranging from 0.311

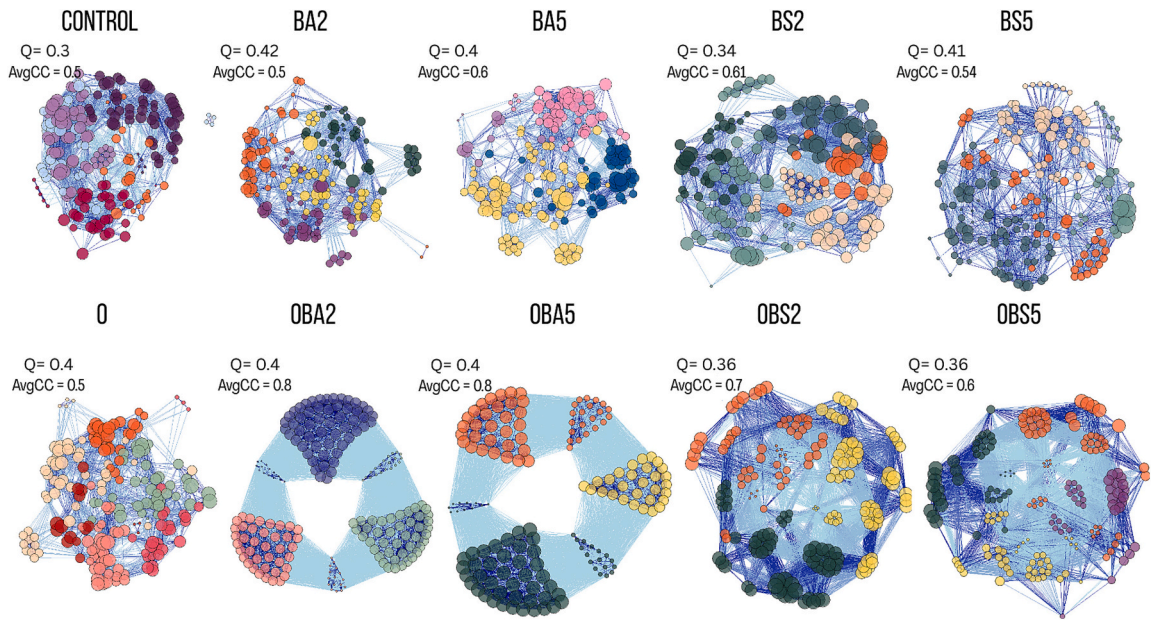

Fig. 5. Co-occurrence networks of soil bacteria for each treatment. Nodes are colored according to modules, and their size reflects the clustering coefficient. Edge color represents interaction strength, with a gradient from light blue (weak interaction) to dark blue (strong interaction), based on the edge weights. Q represents modularity, and AvgCC denotes the average clustering coefficient.

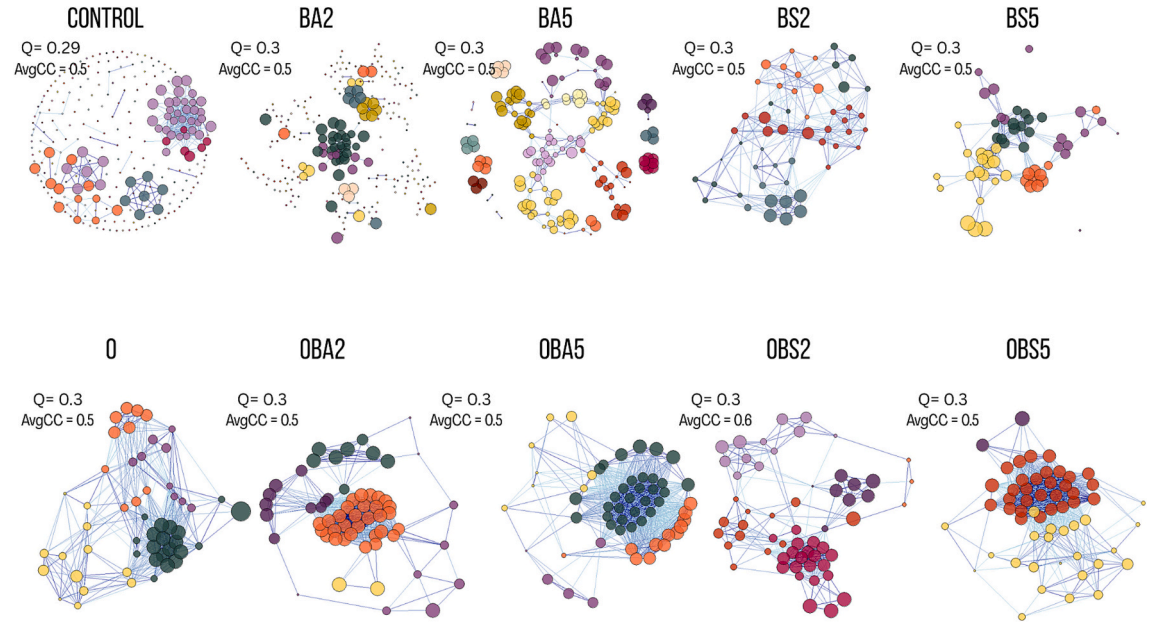

Fig. 6. Co-occurrence networks of soil fungi for each treatment. Nodes are colored according to modules, and their size reflects the clustering coefficient. Edge color represents interaction strength, with a gradient from light blue (weak interaction) to dark blue (strong interaction), based on the edge weights. Q represents modularity, and AvgCC denotes the average clustering coefficient.

(BA2) to 0.813 (OBA2) ($F = 2.6$, $p = 0.006$) (Table S8). The control and BA2 treatments displayed the lowest stability (~0.31), with connectivity dropping from 2.9 to 2.23 and from 2.97 to 2.23, respectively. A similar pattern emerged when examining the effect of targeted node loss through the removal of bridge species—nodes with the highest betweenness centrality (Table S9). Bacterial networks maintained relatively high connectivity after the targeted loss of central taxa, whereas fungal networks showed a sharper decrease in connectivity in both the control and BA2. Notably, these networks also had the lowest initial stability across all treatments. In contrast, treatments such as BA5, OBA2, and OBA5 maintained higher fungal connectivity post-removal (e.g., BA5: 33.75 to 31.4), suggesting that critical interactions within these networks were preserved. Additionally, a significant change in Natural Connectivity (NC) for fungal networks was observed following node removal ($F = 163.4$, $p < 0.001$) (Fig. S3). Notably, after random node removal, NC was consistently higher in fungal networks than after targeted hub removal ($p = 0.0003$). Overall, bacterial networks exhibited higher and more consistent stability across treatments, whereas fungal networks displayed lower and more variable stability values (Tables S8 and S9, Fig. S3).

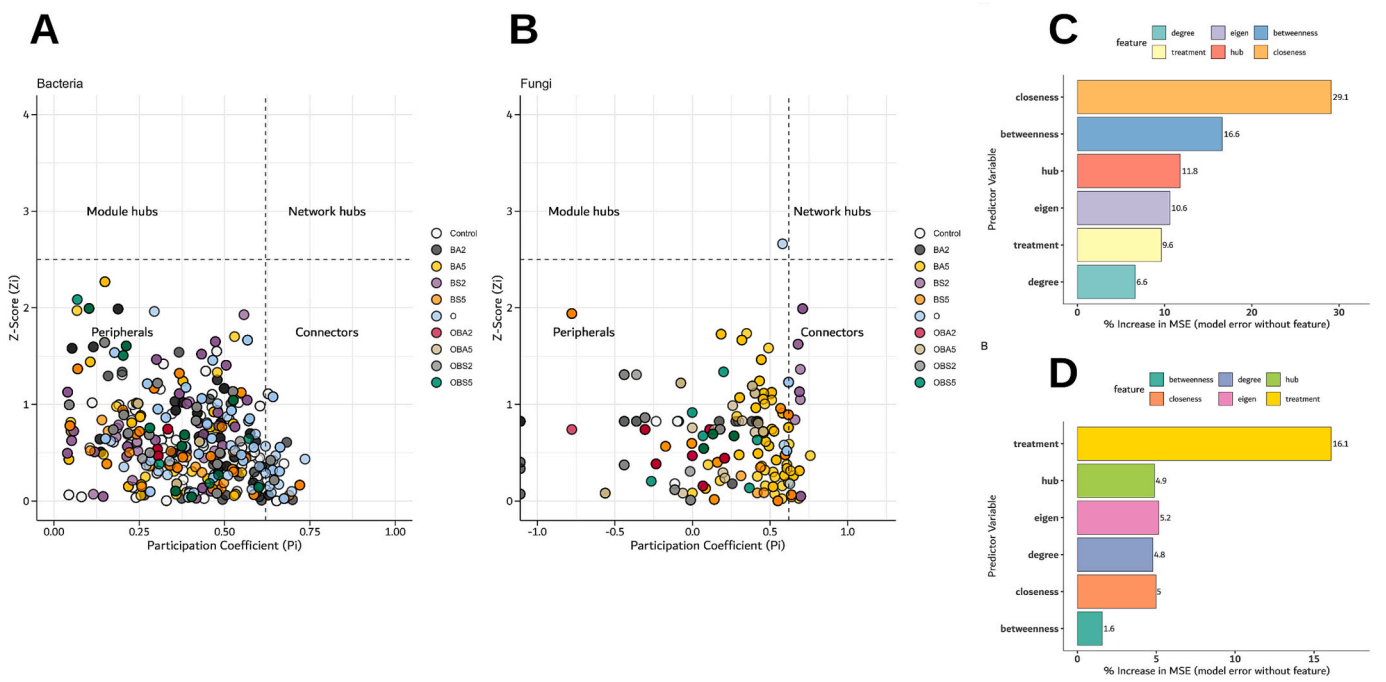

Fig. 7. Topological Analysis of Keystone and Peripheral Taxa Based on Participation Coefficient (Pi) and *Z*-Score (Zi) in bacterial (A) and fungal (B) networks. Panel C and Panel D display the feature importance from Random Forest models applied to bacterial and fungal networks, respectively. The feature importance is measured by the % increase in mean squared error (MSE), which quantifies how much the model's error increases when a particular feature is excluded.

3.5. *Environmental pressure*

Redundancy Analysis (RDA) was performed to assess the extent to which selected environmental variables (i.e., pH, EC, As, Pb, and bioconcentration factor (BCF)) explained the variation in bacterial and fungal community composition (Fig. 8). For the bacterial community, the model explained 28.4 % of the total variance ($p = 0.001$). Among the environmental variables, pH, EC, As, Pb, and BCF were all significant predictors of bacterial community composition (*p*-values of 0.003, 0.002, 0.028, 0.027, and 0.002, respectively). Additionally, the first two RDA axes (RDA1 and RDA2) were also significant ($p = 0.001$ and $p = 0.049$, respectively). Fungal communities showed no significant response to environmental variables ($p = 0.1$), suggesting that unmeasured drivers (e.g., organic exudates) may mediate assembly. EC was the only significant predictor of fungal community composition ($p = 0.03$).

In the SEM model, As and BCF (As) were identified as significant predictors for bacterial α-diversity (measured as H-index) (0.3, CI: 0.07, 0.5; $p = 0.01$ and 1.2, CI: 0.7, 1.6; $p = 0.002$, respectively) (Table S10). EC and the bioconcentration factor (BCF), i.e., the capacity of the plant to accumulate heavy metal/loids in its tissues, were also predictors of

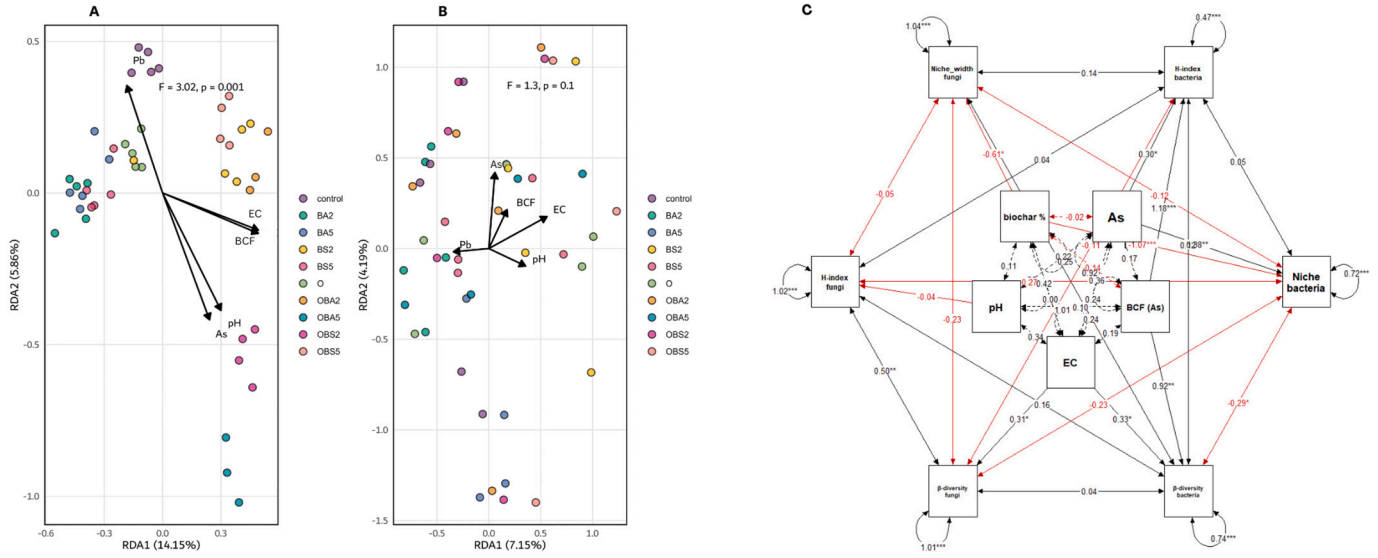

Fig. 8. Redundancy Analysis (RDA) of bacterial (A) and fungal (B) community composition in response to environmental variables (pH, EC, As, Pb, BCF). The sample points are color-coded according to the treatment. Environmental variables are represented by vectors (arrows). The overall model's significance was assessed through a permutation F-test. Panel C represents a structural equation model (SEM) illustrating the direct and indirect effects of environmental stressors on microbial α- and β-diversity. Solid arrows indicate significant pathways ($p < 0.05$), while dashed arrows represent non-significant relationships. Arrow thickness corresponds to standardized path coefficients, with darker edges denoting stronger effects. Asterisks denote statistically significant paths ($p < 0.05$).

changes in bacterial β-diversity (0.3, CI: 0.07, 0.5; $p = 0.01$ and 0.9, CI:0.3,1.4; $p = 0.001$, respectively). Among significant predictors of bacterial niche width, As and biochar concentrations were identified (0.4, CI: 0.1, 0.6; $p = 0.002$ and − 1.07, CI: −1.5, −0.6; $p < 0.0001$, respectively). EC appeared to determine changes in fungal β-diversity (0.3, CI: 0.04, 0.5; $p = 0.02$). Additionally, biochar concentrations were identified as predictors for fungal niche width (−0.6, CI: −1.2, −0.009; $p = 0.04$). We further performed a Spearman correlation analysis between pH, EC, and the abundance of bacterial and fungal taxa (Fig. S4). A positive association with pH was found for many bacterial taxa, among which were *Gemmatimonas, Nitrospira, Ktedonobacter, Sinomonas, Anaeromyxobacter, Anaerospora,* and *Cytophaga*. Furthermore, a positive correlation was observed between the abundances of specific bacterial taxa and EC, including *Fimbriiglobus, Nevskia, Candidatus* Solibacter, *Gemmatimonas, Hyphomicrobium,* and *Gemmata*. The only fungal taxon that showed an increase associated with higher levels of EC was *Chromelosporium*, which was highly abundant in treatments BS2 and BS5. Additionally, we observed that a 5 % biochar concentration significantly affected soil pH, shifting the environment toward alkaline conditions (Fig. 9). Regarding biochar type, treatments incorporating *Solidago gigantea* biochar were associated with markedly high EC values, reaching up to 8000 μS/ cm^{-1}.

4. Discussion

4.1. Biochar dose and type-dependent effects on microbial community structure and assembly

We found that treatments with biochar at 2 % concentrations exhibited higher bacterial diversity compared to the 5 % treatments and the control, which is in accordance with Zhao et al. (2024), who determined the positive effect of biochar at concentrations of up to 2 %

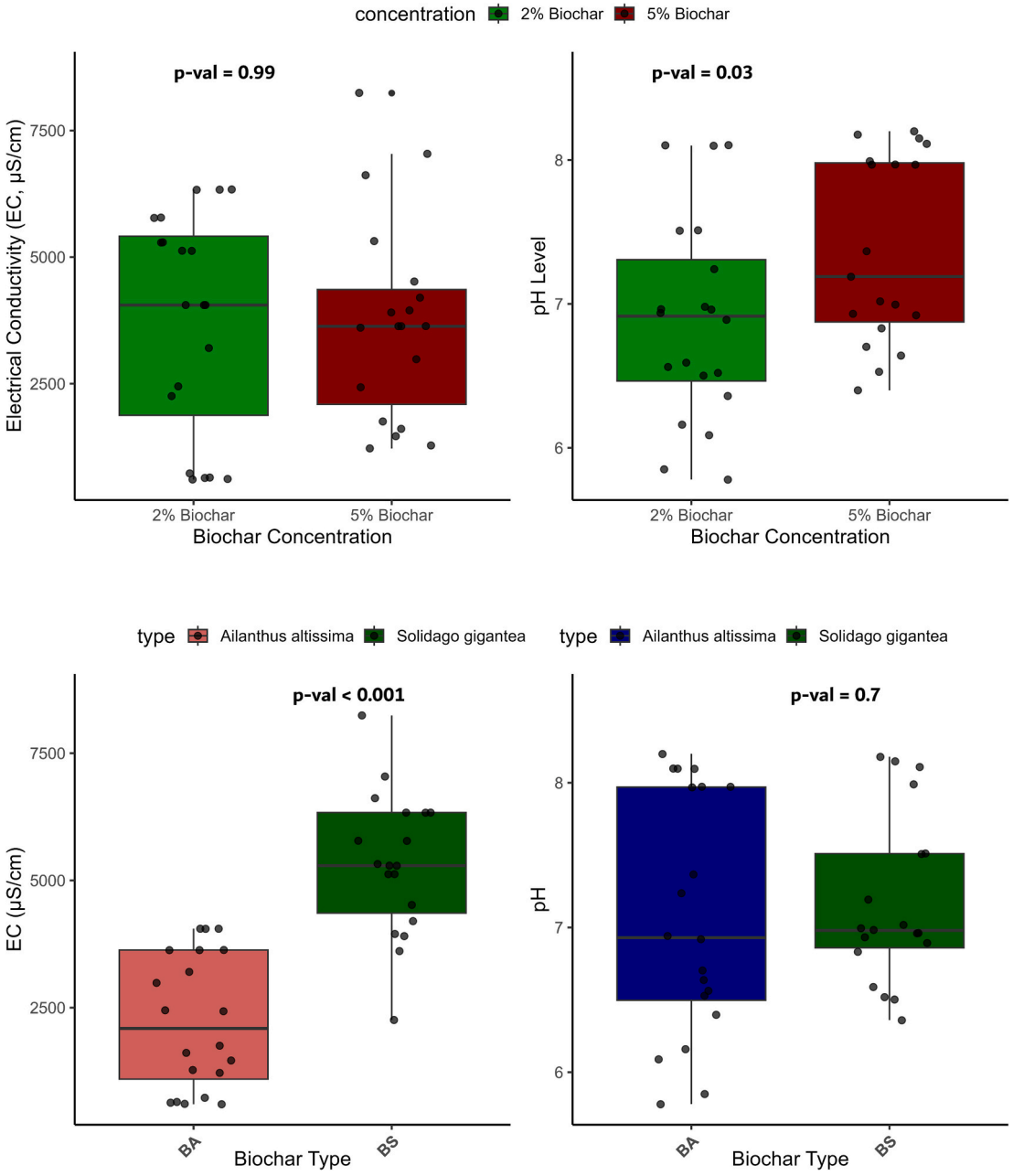

Fig. 9. Effects of biochar type and concentration on soil electrical conductivity (EC) and pH. Boxplots show distributions across treatments, with jittered points representing individual observations. Statistical significance is denoted by *p*-values.

(w/w), whereas higher doses led to a decrease in soil microbial diversity. Zhu et al. (2023) explicitly reported that high-dose biochar (5 %, w/w) applications induced chemical stress in soil microorganisms. The dominance of Cyanobacteria and Bacillota in the control soil may reflect a microbial signature of heavy stress, given that both phyla are commonly associated with the remediation of soils polluted by heavy metals, hydrocarbons, and agrochemicals (Sultana et al., 2022; Li et al., 2020). We observed their decline in amended soil. Therefore, the co-application of biochar with nettle (particularly at 2 %) most likely mitigated such abiotic pressures, resulting in not just increased taxonomic richness but also a more even distribution of microbial taxa. This pattern is consistent with prior observations by Zou et al. (2024) and Bandara et al. (2022), who reported biochar-driven declines in cyanobacterial abundance and the relative abundance of Bacillota. A different picture, however, was observed within fungal communities, which were more responsive to the type of biochar (*Solidago* vs. *Ailanthus*) rather than concentration. *Ailanthus*-derived biochar treatments significantly enriched fungal taxa within the family Coniochaetaceae, whereas *Solidago*-treated plots favored enrichment of fungi belonging to the Pezizaceae family. This finding is consistent with the observation of Muhammad et al. (2014), who found that the type of biochar is positively correlated with the microbial community due to the unique chemical alterations each biochar imparts to the soil. These findings underscore the importance of optimizing both biochar type and dose in supporting microbial diversity in contaminated soils, with significant implications for enhancing phytoremediation strategies.

Biochar co-applied with nettle at both concentrations significantly increased soil pH, which altered community assembly processes. This aligns with Shi et al. (2024), who identified pH as a primary driver of community assembly following the addition of biochar and compost. In our case, the addition of biochar and subsequent increase in pH correlated with an increase in arsenic mobility, and therefore, arsenic could become a factor of selective pressure in the local environment. This was addressed by Zhang et al. (2022) and Wang et al. (2025), who reported a tendency for deterministic selection with increasing heavy metal concentration and the dominance of stochastic processes in less contaminated environments. Another factor that could act as a selective pressure in our study was a drastic increase in EC. The application of biochar to soil has been shown to potentially increase salinity over time, with effects ranging from 0.4 % to 88 %, depending on the feedstock (Brtnicky et al., 2021). This is particularly relevant for high biochar doses; for example, Luo et al. (2017) reported a significant increase in salinity (i.e., reflected in elevated EC values) at biochar concentrations of 5 % and 10 %.

Bacterial community assembly was dominated by stochasticity, whereas deterministic processes influenced fungal community assembly in response to biochar application, consistent with the findings of He et al. (2024). We further observed elevated migration rates within bacterial communities. A high migration rate contributes to heightened community stochasticity, as individuals are more likely to move spatially, resulting in a more homogeneous spatial community structure (Rong et al., 2024; Cao et al., 2024). However, compared to the control, treatments with 5 % biochar co-applied with nettle powder considerably decreased the m rate, suggesting that the amendment's concentrations imposed limitations on dispersal. Generally, lower m rates within fungal communities were in line with their dominance of deterministic patterns. This may be explained by the fact that as eukaryotes with complex life cycles and lower dispersal potential, fungi are more constrained by environmental filters than by processes such as drift or dispersal. For example, Kivlin et al. (2011) found that across a regional landscape, soil fungal communities were shaped more by environmental conditions than by limitations in their ability to disperse. It is important to note that beyond the selected environmental variables, both the RDA and SEM models explained a moderate proportion of variance, whereas the fungal model was not statistically significant. This suggests two possibilities: either the fungal community composition was shaped more by biotic interactions than by soil physicochemical factors or important environmental predictors were omitted from the analysis. Several studies highlight the critical role of plant-microbe interactions, root exudates, and microclimate (e.g., soil moisture and temperature), as well as spatial heterogeneity in determining microbial community structure and function (Zhalnina et al., 2018; Jacoby and Kopriva, 2019; Ma et al., 2022; Wu et al., 2024). We, therefore, highly recommend incorporating such variables in future studies to achieve a more comprehensive understanding.

4.2. Niche variations of soil bacterial and fungal community in response to environmental disturbance

Bacterial communities in soils amended with stinging nettle and biochar exhibited increased niche width, especially in combination treatments applied at a 2 % concentration. Resource availability mediates niche differentiation (Lin et al., 2021). The niche responses of bacteria and fungi are often kingdom-specific because of their contrasting nutrient demands (e.g., C:N:P stoichiometry) and differing sensitivities to abiotic factors (e.g., temperature, pH, moisture, and oxygen availability) (Wang and Kuzyakov, 2024). Consequently, even minor changes in these factors can strongly alter microbial metabolic strategies. Biochar's porous structure provides a physical template that influences microbial distribution, not only by creating resource gradients but also by offering a suitable habitat for microbial colonization (Xiang et al., 2022; Bolan et al., 2023). It remains unclear in our study whether the observed increase in bacterial niche breadth reflects actual niche expansion or simply a shift in the realized niche due to changes in the physical environment, as we did not directly test resource use expansion. Biochar may increase abiotic heterogeneity by creating new microsites, which, according to ecological theory (Van Valen, 1965; Roughgarden, 1972; Yates et al., 2022) could reduce the likelihood of direct competition by allowing taxa to persist in distinct microhabitats or occupy previously inaccessible niches. Such processes may help explain the observed decrease in species co-occurrences.

In contrast, we observed a reduction in fungal niche width in response to amendments, consistent with conditions that support the prevalence of specialists, which are often keystone taxa crucial for community stability (Ma et al., 2025). For fungi, which disperse over broader spatial scales than bacteria, the addition of the investigated amendments may have homogenized the environment compared to the control, thereby intensifying competition and favoring specialists that are better adapted to compete in a more uniform habitat. For example, according to the "specialization-disturbance" hypothesis, disturbances are typically believed to have a negative impact on specialists, whereas generalists are thought to benefit from them (Vázquez and Simberloff, 2002). However, this was not the case for fungal communities in our study, as specialists dominated the amended soil. This may partially explain why the fungal community appeared more fragile in the face of disturbance compared to that of bacteria. Niche breadth is often used to infer a species' tolerance to changing conditions, and specialists, having more restricted distributions than generalists (Brown, 1984), are more vulnerable to extinction (Vázquez and Simberloff, 2002; Malard et al., 2022).

We identified increased niche overlap among fungal species following the amendment treatments compared to the control. Although this could be indicative of intensified competition due to environmental homogenization, it may also reflect functional compensation, as described by Yachi and Loreau (1999). In the case of the latter, according to Hunting et al. (2015), this would suggest that species with niche overlaps may play distinct ecological roles, thereby reducing direct competition through functional differentiation rather than direct competitive exclusion. It is tempting to interpret the observed niche overlap as a result of environmental filtering, where similar species persist under the same environmental constraints. However, recent perspectives from coexistence theory caution against such rigid

interpretations. As Cadotte and Tucker (2017) argue, environmental impacts on intrinsic growth rates can lead to competitive exclusion well before environmental conditions themselves cause mortality, making competition a more immediate and likely structuring force than strict abiotic filtering.

4.3. Network stability and robustness

Biochar at 2 % concentrations co-applied with nettle powder enhanced network complexity and robustness in amended plots. The unique effect of nettle co-application likely reflects its organic nutrient contribution (Devkota et al., 2022). However, compared to bacterial networks, fungi exhibited fewer negative associations. While species co-occurrence alone does not confirm ecological interactions, we might approach interpretability when integrated with other metrics. In our case, the dominance of deterministic assembly reduced fungal niche breadth, and the decreased species co-occurrence could indicate the restructuring of the fungal community, favoring stress-tolerant specialists (Kajihara and Hynson, 2024). In our study, Ascomycota was shown to be the most prevalent fungal phylum across all treatments. This phylum has been found to thrive in the presence of organic and inorganic pollutants, such as heavy metals and petroleum-derived contaminants, by secreting extracellular enzymes primarily used for cellulose and lignin decomposition (e.g., cytochrome P450, lignin peroxidase, manganese peroxidase, and laccase) (Harms et al., 2011), as well as for transforming heavy metal ions into their less toxic forms (Okrasińska et al., 2022). Supporting this, experiments performed on multi-polluted, post-industrial sites have consistently reported that fungal communities in these types of environments are dominated by the phylum Ascomycota (Thion et al., 2012; Bourceret et al., 2016). Sun et al. (2022) and Gai et al. (2024) reported that biochar amendments increased the positive associations within microbial networks. Bello et al. (2021) interpreted a similar pattern of the increase in fungal links as indicative of a "more cooperative state" within the community.

The treatments with 2 % biochar demonstrated more nodes, edges, and a higher *p_rc* index in fungal networks compared to the 5 % treatments. The *p_rc* index quantifies the critical proportion of randomly removed nodes required to fragment the network, with higher values indicating greater structural robustness to random disturbances (Liu et al., 2017). Robust networks are those capable of withstanding significant disruptions without collapsing, a concept widely agreed upon in the literature (Fan et al., 2018; Tipton et al., 2018; Yuan et al., 2021; Wu et al., 2021; Li et al., 2023; Kajihara and Hynson, 2024), In turn, higher network robustness correlates with enhanced community-level stability. Treatments with *Ailanthus*-derived biochar demonstrated the highest average connectivity and resilience to hub loss, maintaining network integrity under disturbance compared to networks in *Solidago* treatments, which exhibited the highest EC values and potentially compromised stability. The bacterial network across treatments did not exhibit module hubs, indicating that it did not rely on hubs for connectivity. This was not the case for fungal networks, where a structural feature (i.e., module hub) emerged and, thus, indicated heightened vulnerability, as such hubs are disproportionately important in structuring microbial communities (Gao et al., 2022). The results of our Random Forest analysis align with network-based resilience theory, which emphasizes the importance of nodes that facilitate rapid communication or exert influence across a network in maintaining its cohesion (Gao et al., 2022; Rawstern et al., 2025). In the context of both bacterial and fungal networks, centrality measures such as closeness and eigenvector centrality were found to predict changes in network stability. For example, species with the highest closeness centrality are considered key players, as they can quickly interact with many network components (Pavlopoulos et al., 2011; Codello et al., 2023). Segarra and Ribeiro (2016) noted that betweenness centrality is less stable and can be significantly influenced by noise in the network data, unlike metrics such as degree, closeness, and eigenvector centrality. In our analysis, the structural stability in bacterial networks appears to derive from distributed centrality rather than being concentrated in a few hubs. This type of network organization reflects a form of internal regulation and cohesion, often termed a mature, self-organizing system (Levin, 2005). For fungal networks, node stability is primarily driven by treatment identity rather than internal network topology. Thus, they are more likely to be externally regulated and sensitive to changes in resource availability or habitat conditions. Moreover, in our study, although all fungal networks were considered to be small-world, none of them were modular ($Q < 0.4$). For example, as shown by Buldyrev et al. (2010), interdependent systems (i.e., those that lack compartmentalization) can lead to cascading failures, where the failure of a very small fraction of nodes may result in the complete fragmentation of a system. By contrast, a modular network prevents cascading disruptions from spreading through the whole system because the connections between modules are limited, and therefore, it acts as a buffer, containing disturbances within isolated sections of the network (Namdar et al., 2024). Guo et al. (2022) also stated that high modularity implies less interdependence among the taxa (nodes) and more divergent functional groups. In bacterial networks, all treatments with *Ailanthus-derived biochar* exhibited *a* modular structure, higher average connectivity, and a clustering coefficient, all of which indicate a more robust system compared to fungal networks.

5. Conclusion

In a context where the management of invasive alien species remains challenging and an unresolved global challenge, our findings indicate that their biomass can be turned into a useful resource for soil remediation. In this way, we show the potential of waste material to be valorized while at the same time contributing to phytoremediation outcomes. In here, we analyzed community assembly, niche dynamics, and network robustness, moving past the conventional emphasis on diversity indices or taxonomic composition alone, and this allows us to better comprehend belowground microbial responses. Also, our data reveal that higher amendment levels (5 % biochar) are not necessarily beneficial. It did not only constrain fungal community resilience but also produced marked physicochemical changes, such as strong alkalinization ($pH > 7$) and extreme increases in electrical conductivity ($EC > 6000$ μS/cm). Such conditions may be detrimental to plant performance and are rarely feasible in field applications. By contrast, inputs of 2 % biochar applied together with stinging nettle proved more effective in supporting microbial diversity, resilience, and stability. This challenges the common assumption that "more is better" and points out to dose-dependent thresholds which are critical to design sustainable phytoremediation strategies in practice. Biochar amendments represent a promising approach for mitigating soil pollution; however, their effects on soil microbial communities are context-dependent and vary across microbial taxa. In polluted soils amended with biochar, bacterial communities were predominantly structured by stochastic processes, whereas fungal communities exhibited greater specialization and were primarily governed by deterministic processes. These contrasting assembly mechanisms imply that fungal communities may be managed through the regulation of biotic interactions and soil physicochemical properties, while bacterial communities are more likely to respond to proactive interventions. Consequently, phytoremediation initiatives should establish clear priorities and design strategies that integrate these microbial dynamics with practical considerations such as labor availability and financial resources.

CRediT authorship contribution statement

Snezhana Mourouzidou: Writing – original draft, Formal analysis, Investigation, Data curation. **Magkdi Mola:** Writing – review & editing, Investigation, Resources. **Alex Ceriani:** Methodology, Writing – review & editing, Data curation. **Spiros Papakostas:** Writing – review & editing, Methodology. **Marta Sena-Velez:** Writing – review & editing.

Efimia M. Papatheodorou: Writing – review & editing, Methodology. **Antonio Montagnoli:** Writing – review & editing, Resources, Supervision. **Domenico Morabito:** Writing – review & editing, Methodology, Validation, Resources, Supervision. **Nikolaos Monokrousos:** Writing – review & editing, Methodology, Validation, Supervision, Resources, Conceptualization.

Funding statement

This research did not receive any specific grant from funding agencies in the public, commercial, or not-for-profit sectors.

Declaration of competing interest

The authors declare that they have no known competing financial interests or personal relationships that could have appeared to influence the work reported in this paper.

Appendix A. Supplementary data

Supplementary data to this article can be found online at https://doi.org/10.1016/j.scitotenv.2025.180693.

Data availability

Data will be made available on request.

References

Adirianto, B., Bachtiar, T., 2023. Effect of biochar in soil on microbial diversity: a meta-analysis. IOP Conf. Ser. Earth Environ. Sci. 1263, 012047. https://doi.org/10.1088/1755-1315/1263/1/012047.

Aqeel, M., Ran, J., Hu, W., Irshad, M.K., Dong, L., Akram, M.A., Eldesoky, G.E., Aljuwayid, A.M., Chuah, L.F., Deng, J., 2023. Plant-soil-microbe interactions in maintaining ecosystem stability and coordinated turnover under changing environmental conditions. Chemosphere 318, 137924. https://doi.org/10.1016/j.chemosphere.2023.137924.

Arulselvan, A., Manimuthu, M., Narayanaswamy, R., 2024. Molecular docking analysis of selected Urtica dioica constituents as human carbonic anhydrase II (hCA-II), human 11 beta-hydroxysteroid dehydrogenases type 1 (h11beta-HSD1), and human dual specificity phosphatase (hCDC25B) inhibitory agents. Cureus 16. https://doi.org/10.7759/cureus.53886.

Bandara, T., Krohn, C., Jin, J., Chathurika, J.B.A.J., Franks, A., Xu, J., Potter, I.D., Tang, C., 2022. The effects of biochar aging on rhizosphere microbial communities in cadmium-contaminated acid soil. Chemosphere 303, 135153. https://doi.org/10.1016/j.chemosphere.2022.135153.

Baas Becking, L.G.M., 1934. Geobiologie of Inleiding Tot de Milieukunde. W.P. Van Stockum & Zoon, The Hague.

Bello, A., Wang, B., Zhao, Y., Yang, W., Ogundeji, A., Deng, L., Egbeagu, U.U., Yu, S., Zhao, L., Li, D., Xu, X., 2021. Composted biochar affects structural dynamics, function and co-occurrence network patterns of fungi community. Sci. Total Environ. 775, 145672. https://doi.org/10.1016/j.scitotenv.2021.145672.

Benjamini, Y., Hochberg, Y., 1995. Controlling the false discovery rate: a practical and powerful approach to multiple testing. J. Roy. Stat. Soc. Ser. B 57, 289–300. https://doi.org/10.1111/j.2517-6161.1995.tb02031.x.

Bici, M., Halili, J., Bislimi, K., Zogaj, M., Mazreku, I., 2023. Bioaccumulation and biomagnification from soil to nettle-snail and extension heavy metal pollution of mining activity "ferronikel" in Drenas. Ecol. Eng. Environ. Technol. 24, 358–366. https://doi.org/10.12912/27197050/174259.

Bolan, S., Hou, D., Wang, L., Hale, L., Egamberdieva, D., Tammeorg, P., Li, R., Wang, B., Xu, J., Wang, T., Sun, H., Padhye, L.P., Wang, H., Siddique, K.H.M., Rinklebe, J., Kirkham, M.B., Bolan, N., 2023. The potential of biochar as a microbial carrier for agricultural and environmental applications. Sci. Total Environ. 886, 163968. https://doi.org/10.1016/j.scitotenv.2023.163968.

Bontemps, Z., Moënne-Loccoz, Y., Hugoni, M., 2024. Stochastic and deterministic assembly processes of microbial communities in relation to natural attenuation of black stains in Lascaux Cave. mSystems 9. https://doi.org/10.1128/msystems.01233-23 e01233-23.

Bourceret, A., Cébron, A., Tisserant, E., Poupin, P., Bauda, P., Beguiristain, T., Leyval, C., 2016. The bacterial and fungal diversity of an aged PAH- and heavy metal-contaminated soil is affected by plant cover and edaphic parameters. Microb. Ecol. 71, 711–724. https://doi.org/10.1007/s00248-015-0682-8.

Brown, J.H., 1984. On the relationship between abundance and distribution of species. Am. Nat. 124 (2), 255–279. https://doi.org/10.1086/284267.

Brtnicky, M., Datta, R., Holatko, J., Bielska, L., Gusiatin, Z.M., Kucerik, J., Hammerschmiedt, T., Danish, S., Radziemska, M., Mravcova, L., Fahad, S., Kintl, A., Sudoma, M., Ahmed, N., Pecina, V., 2021. A critical review of the possible adverse effects of biochar in the soil environment. Sci. Total Environ. 796, 148756. https://doi.org/10.1016/j.scitotenv.2021.148756.

Büchi, L., Vuilleumier, S., 2014. Coexistence of specialist and generalist species is shaped by dispersal and environmental factors. Am. Nat. 183, 612–624. https://doi.org/10.1086/675756.

Buldyrev, S.V., Parshani, R., Paul, G., Stanley, H.E., Havlin, S., 2010. Catastrophic cascade of failures in interdependent networks. Nature 464, 1025–1028. https://doi.org/10.1038/nature08932.

Cadotte, M.W., Tucker, C.M., 2017. Should environmental filtering be abandoned? Trends Ecol. Evol. 32, 429–437. https://doi.org/10.1016/j.tree.2017.03.004.

Cao, J., Yang, X., Guo, M., Wu, Y., Wang, C., 2024. Reclamation of abandoned cropland switches fungal community assembly from deterministic to stochastic processes. Sci. Total Environ. 951, 175494. https://doi.org/10.1016/j.scitotenv.2024.175494.

Ceriani, A., Chafik, Y., Miali, A., Bourgerie, S., Dalle Fratte, M., Cerabolini, B.E.L., Morabito, D., Montagnoli, A., 2025. Remediating heavy metal-contaminated soil through invasive alien plant-derived biochar and stinging nettle powder. Chemosphere 380, 144435. https://doi.org/10.1016/j.chemosphere.2025.144435.

Clarke, K.R., 1993. Non-parametric multivariate analyses of changes in community structure. Aust. J. Ecol. 18, 117–143. https://doi.org/10.1111/j.1442-9993.1993.tb00438.x.

Clavel, J., Julliard, R., Devictor, V., 2011. Worldwide decline of specialist species: toward a global functional homogenization? Front. Ecol. Environ. 9, 222–228. https://doi.org/10.1890/080216.

Codello, A., Hose, G.C., Chariton, A., 2023. Microbial co-occurrence networks as a biomonitoring tool for aquatic environments: a review. Mar. Freshw. Res. 74, 409–422. https://doi.org/10.1071/MF22045.

Coyte, K.Z., Schluter, J., Foster, K.R., 2015. The ecology of the microbiome: networks, competition, and stability. Science 350, 663–666. https://doi.org/10.1126/science.aad2602.

Deng, Y., Jiang, Y.-H., Yang, Y., He, Z., Luo, F., Zhou, J., 2012. Molecular ecological network analyses. BMC Bioinf. 13, 113. https://doi.org/10.1186/1471-2105-13-113.

Deshoux, M., Sadet-Bourgeteau, S., Gentil, S., Prévost-Bouré, N.C., 2023. Effects of biochar on soil microbial communities: a meta-analysis. Sci. Total Environ. 902, 166079. https://doi.org/10.1016/j.scitotenv.2023.166079.

Devkota, H.P., Paudel, K.R., Khanal, S., Baral, A., Panth, N., Adhikari-Devkota, A., Jha, N.K., Das, N., Singh, S.K., Chellappan, D.K., Dua, K., Hansbro, P.M., 2022. Stinging nettle (*Urtica dioica* L.): nutritional composition, bioactive compounds, and food functional properties. Molecules 27, 5219. https://doi.org/10.3390/molecules27165219.

Dunne, J.A., Williams, R.J., Martinez, N.D., 2002. Network structure and biodiversity loss in food webs: robustness increases with connectance. Ecol. Lett. 5, 558–567. https://doi.org/10.1046/j.1461-0248.2002.00354.x.

Elmeknassi, M., Elghali, A., de Carvalho, H.W.P., Laamrani, A., Benzaazoua, M., 2024. A review of organic and inorganic amendments to treat saline-sodic soils: emphasis on waste valorization for a circular economy approach. Sci. Total Environ. 921, 171087. https://doi.org/10.1016/j.scitotenv.2024.171087.

Epskamp, S., 2015. semPlot: unified visualizations of structural equation models. Struct. Equ. Model. Multidiscip. J. 22 (3), 474–483. https://doi.org/10.1080/10705511.2014.937847.

Ertan, B., Efe, D., 2019. The adsorption performance of Urtica dioica on the removal of cadmium from aqueous solutions. Asian J. Biotechnol. Genet. Eng. 183–189.

Fan, K., Weisenhorn, P., Gilbert, J.A., Chu, H., 2018. Wheat rhizosphere harbors a less complex and more stable microbial co-occurrence pattern than bulk soil. Soil Biol. Biochem. 125, 251–260. https://doi.org/10.1016/j.soilbio.2018.07.022.

Gai, X., Li, X., Xing, W., Zhang, X., Chen, G., 2024. Mechanism insights into amendments enhanced dendroremediation for Cd and Zn-polluted soil: bacterial co-occurrence networks' complexity and stability. Geoderma 451, 117088. https://doi.org/10.1016/j.geoderma.2024.117088.

Gao, C., Xu, L., Montoya, L., Yang, Y., Wu, M., Dang, P., Xu, J., Bai, Y., 2022. Co-occurrence networks reveal more complexity than community composition in resistance and resilience of microbial communities. Nat. Commun. 13, 3867. https://doi.org/10.1038/s41467-022-31343-y.

Guo, B., Zhang, L., Sun, H., Gao, M., Yu, N., Zhang, Q., Mou, A., Liu, Y., 2022. Microbial co-occurrence network topological properties link with reactor parameters and reveal importance of low-abundance genera. NPJ Biofilms Microbiomes 8, 1–13. https://doi.org/10.1038/s41522-021-00263-y.

Guseva, K., Darcy, S., Simon, E., Alteio, L.V., Montesinos-Navarro, A., Kaiser, C., 2022. From diversity to complexity: microbial networks in soils. Soil Biol. Biochem. 169, 108604. https://doi.org/10.1016/j.soilbio.2022.108604.

Harms, H., Schlosser, D., Wick, L.Y., 2011. Untapped potential: exploiting fungi in bioremediation of hazardous chemicals. Nat. Rev. Microbiol. 9, 177–192. https://doi.org/10.1038/nrmicro2519.

He, C., Harindintwali, J.D., Cui, H., Zheng, W., Zhu, Q., Chang, S.X., Wang, F., Yang, J., 2024. Decoupled fungal and bacterial functional responses to biochar amendment drive rhizosphere priming effect on soil organic carbon mineralization. Biochar 6, 84. https://doi.org/10.1007/s42773-024-00376-5.

Hernandez, D.J., David, A.S., Menges, E.S., Searcy, C.A., Afkhami, M.E., 2021. Environmental stress destabilizes microbial networks. ISME J. 15 (6), 1722–1734. https://doi.org/10.1038/s41396-020-00882-x.

Hunting, E.R., Vijver, M.G., van der Geest, H.G., Mulder, C., Kraak, M.H.S., Breure, A.M., Admiraal, W., 2015. Resource niche overlap promotes stability of bacterial community metabolism in experimental microcosms. Front. Microbiol. 6. https://doi.org/10.3389/fmicb.2015.00105.

Jacoby, R.P., Kopriva, S., 2019. Metabolic niches in the rhizosphere microbiome: new tools and approaches to analyse metabolic mechanisms of plant–microbe nutrient exchange. J. Exp. Bot. 70, 1087–1094. https://doi.org/10.1093/jxb/ery438.
Ji, P., Wilson, M., 2002. Assessment of the importance of similarity in carbon source utilization profiles between the biological control agent and the pathogen in biological control of bacterial speck of tomato. Appl. Environ. Microbiol. 68, 4383–4389. https://doi.org/10.1128/AEM.68.9.4383-4389.2002.
Jiang, W., Fan, T., Li, C., Zhang, C., Zhang, T., Luo, Z., 2024. Comprehensive analysis of network robustness evaluation based on convolutional neural networks with spatial pyramid pooling. Chaos, Solitons Fractals 184, 115023. https://doi.org/10.1016/j.chaos.2024.115023.
Jiang, Y., Huang, H., Tian, Y., Yu, X., Li, X., 2021. Stochasticity versus determinism: microbial community assembly patterns under specific conditions in petrochemical activated sludge. J. Hazard. Mater. 407, 124372. https://doi.org/10.1016/j.jhazmat.2020.124372.
Jun, W.U., Barahona, M., Yue-Jin, T.a.N., Hong-Zhong, D., 2010. Natural connectivity of complex networks. Chin. Phys. Lett. 27, 078902–078902. https://doi.org/10.1088/0256-307X/27/7/078902.
Kajihara, K.T., Hynson, N.A., 2024. Networks as tools for defining emergent properties of microbiomes and their stability. Microbiome 12, 184. https://doi.org/10.1186/s40168-024-01868-z.
Karimi, B., Maron, P.A., Chemidlin-Prevost Boure, N., Bernard, N., Gilbert, D., Ranjard, L., 2017. Microbial diversity and ecological networks as indicators of environmental quality. Environ. Chem. Lett. 15, 265–281. https://doi.org/10.1007/s10311-017-0614-6.
Kerner, P., Struhs, E., Mirkouei, A., Aho, K., Lohse, K.A., Dungan, R.S., You, Y., 2023. Microbial responses to biochar soil amendment and influential factors: a three-level meta-analysis. Environ. Sci. Technol. 57, 19838–19848. https://doi.org/10.1021/acs.est.3c04201.
Kivlin, S., Hawkes, C., Treseder, K., 2011. Global diversity and distribution of arbuscular mycorrhizal fungi. Soil Biol. Biochem. 43, 2294–2303. https://doi.org/10.1016/j.soilbio.2011.07.012.
Kruskal, J.B., 1964. Nonmetric multidimensional scaling: a numerical method. Psychometrika 29, 115–129. https://doi.org/10.1007/BF02289694.
Kuhn, M., 2008. Building predictive models in R using the caret package. J. Stat. Softw. 28, 1–26. https://doi.org/10.18637/jss.v028.i05.
Lebrun, M., Macri, C., Miard, F., Hattab-Hambli, N., Motelica-Heino, M., Morabito, D., Bourgerie, S., 2017. Effect of biochar amendments on As and Pb mobility and phytoavailability in contaminated mine technosols phytoremediated by *Salix*. J. Geochem. Explor. 182, 149–156. https://doi.org/10.1016/j.gexplo.2016.11.016.
Legendre, P., Legendre, L., 2012. *Numerical Ecology*, 3rd, English ed. Elsevier, Amsterdam.
Levin, S.A., 2005. Self-organization and the emergence of complexity in ecological systems. BioScience 55, 1075–1079. https://doi.org/10.1641/0006-3568(2005)055[1075:SATEOC]2.0.CO;2.
Levins, R., 1968. Evolution in Changing Environments: Some Theoretical Explorations. Princeton University Press, Princeton.
Li, Q., You, P., Hu, Q., Leng, B., Wang, J., Chen, J., Wan, S., Wang, B., Yuan, C., Zhou, R., Ouyang, K., 2020. Effects of co-contamination of heavy metals and total petroleum hydrocarbons on soil bacterial community and function network reconstitution. Ecotoxicol. Environ. Saf. 204, 111083. https://doi.org/10.1016/j.ecoenv.2020.111083.
Li, R., Wang, B., Niu, A., Cheng, N., Chen, M., Zhang, X., Yu, Z., Wang, S., 2022. Application of biochar immobilized microorganisms for pollutants removal from wastewater: a review. Sci. Total Environ. 837, 155563. https://doi.org/10.1016/j.scitotenv.2022.155563.
Li, Z., Sun, L., Liu, S., Lei, P., Wang, R., Li, S., Gu, Y., 2023. Interkingdom network analyses reveal microalgae and protostomes as keystone taxa involved in nutrient cycling in large freshwater lake sediment. FEMS Microbiol. Ecol. 99, fiad111. https://doi.org/10.1093/femsec/fiad111.
Lin, Q., Li, L., Adams, J., Heděnec, P., Tu, B., Li, C., Tongtong, L., Li, X., 2021. Nutrient resource availability mediates niche differentiation and temporal co-occurrence of soil bacterial communities. Appl. Soil Ecol. 163, 103965. https://doi.org/10.1016/j.apsoil.2021.103965.
Ling, N., Wang, T., Kuzyakov, Y., 2022. Rhizosphere bacteriome structure and functions. Nat. Commun. 13, 836. https://doi.org/10.1038/s41467-022-28448-9.
Liu, C., Cui, Y., Li, X., Yao, M., 2021. microeco: an R package for data mining in microbial community ecology. FEMS Microbiol. Ecol. 97, fiaa255. https://doi.org/10.1093/femsec/fiaa255.
Liu, J., Zhou, M., Wang, S., Liu, P., 2017. A comparative study of network robustness measures. Front. Comput. Sci. 11, 568–584. https://doi.org/10.1007/s11704-016-6108-z.
Liu, S., Yu, H., Yu, Y., Huang, J., Zhou, Z., Zeng, J., Chen, P., Xiao, F., He, Z., Yan, Q., 2022. Ecological stability of microbial communities in Lake Donghu regulated by keystone taxa. Ecol. Indic. 136, 108695. https://doi.org/10.1016/j.ecolind.2022.108695.
Liu, S., Shi, Y., Sun, M., Huang, D., Shu, W., Ye, M., 2023. The community assembly for understanding the viral-assisted response of bacterial community to Cr-contamination in soils. J. Hazard. Mater. 441, 129975. https://doi.org/10.1016/j.jhazmat.2022.129975.
Lomaglio, T., Hattab-Hambli, N., Miard, F., Lebrun, M., Nandillon, R., Trupiano, D., Scippa, G.S., Gauthier, A., Motelica-Heino, M., Bourgerie, S., Morabito, D., 2018. Cd, Pb, and Zn mobility and (bio)availability in contaminated soils from a former smelting site amended with biochar. Environ. Sci. Pollut. Res. Int. 25, 25744–25756. https://doi.org/10.1007/s11356-017-9521-4.
Luo, X., Liu, G., Xia, Y., Chen, L., Jiang, Z., Zheng, H., Wang, Z., 2017. Use of biochar-compost to improve properties and productivity of the degraded coastal soil in the Yellow River Delta, China. J. Soils Sediments 17, 780–789. https://doi.org/10.1007/s11368-016-1361-1.
Ma, G., Shi, M., Li, Y., Wang, S., Zeng, X., Jia, Y., 2025. Diverse adaptation strategies of generalists and specialists to metal and salinity stress in the coastal sediments. Environ. Res. 271, 121073. https://doi.org/10.1016/j.envres.2025.121073.
Ma, L., Liu, L., Lu, Y., Chen, L., Zhang, Z., Zhang, H., Wang, X., Shu, L., Yang, Q., Song, Q., Peng, Q., Yu, Z., Zhang, J., 2022. When microclimates meet soil microbes: temperature controls soil microbial diversity along an elevational gradient in subtropical forests. Soil Biol. Biochem. 166, 108566. https://doi.org/10.1016/j.soilbio.2022.108566.
Malard, L.A., Mod, H.K., Guex, N., Broennimann, O., Yashiro, E., Lara, E., Mitchell, E.A. D., Niculita-Hirzel, H., Guisan, A., 2022. Comparative analysis of diversity and environmental niches of soil bacterial, archaeal, fungal and protist communities reveal niche divergences along environmental gradients in the Alps. Soil Biol. Biochem. 169, 108674. https://doi.org/10.1016/j.soilbio.2022.108674.
Mazzurco-Miritana, V., Passatore, L., Zacchini, M., Pietrini, F., Peruzzi, E., Carloni, S., Rolando, L., Garbini, G.L., Barra Caracciolo, A., Silvani, V., Moscatelli, M.C., Marabottini, R., Massaccesi, L., Marinari, S., Nogués, I., 2025. Promoting the remediation of contaminated soils using biochar in combination with bioaugmentation and phytoremediation techniques. Sci. Rep. 15, 11231. https://doi.org/10.1038/s41598-025-93879-5.
McMurdie, P.J., Holmes, S., 2013. phyloseq: an R package for reproducible interactive analysis and graphics of microbiome census data. PLoS One 8, e61217. https://doi.org/10.1371/journal.pone.0061217.
Mills, S., Ijaz, U.Z., Lens, P.N.L., 2025. Environmental instability reduces shock resistance by enriching specialist taxa with distinct two component regulatory systems. npj Biofilms Microbiomes 11, 1–15. https://doi.org/10.1038/s41522-025-00679-w.
Muhammad, N., Dai, Z., Xiao, K., Meng, J., Brookes, P.C., Liu, X., Wang, H., Wu, J., Xu, J., 2014. Changes in microbial community structure due to biochars generated from different feedstocks and their relationships with soil chemical properties. Geoderma 226–227, 270–278. https://doi.org/10.1016/j.geoderma.2014.01.023.
Muller, E.E.L., 2019. Determining microbial niche breadth in the environment for better ecosystem fate predictions. mSystems 4. https://doi.org/10.1128/msystems.00080-19.
Namdar, J., Blackhurst, J., Zhao, K., Song, S., 2024. Cascading disruptions: impact of modularity and nexus supplier predictions. J. Supply Chain Manag. 60, 18–38. https://doi.org/10.1111/jscm.12326.
Ning, D., Deng, Y., Tiedje, J.M., Zhou, J., 2019. A general framework for quantitatively assessing ecological stochasticity. Proc. Natl. Acad. Sci. 116, 16892–16898. https://doi.org/10.1073/pnas.1904623116.
Okrasińska, A., Decewicz, P., Majchrowska, M., Dziewit, L., Muszewska, A., Dolatabadi, S., Kruszewski, Ł., Błocka, Z., Pawłowska, J., 2022. Marginal lands and fungi – linking the type of soil contamination with fungal community composition. Environ. Microbiol. 24, 3809–3825. https://doi.org/10.1111/1462-2920.16007.
Oksanen, J., Simpson, G.L., Blanchet, F.G., Kindt, R., Legendre, P., Minchin, P.R., O'Hara, R.B., Solymos, P., Stevens, M.H.H., Szoecs, E., Wagner, H., Barbour, M., Bedward, M., Bolker, B., Borcard, D., Carvalho, G., et al., 2022. *vegan*: Community Ecology Package. R Package Version 2.6-4. https://CRAN.R-project.org/package=vegan.
Olden, J.D., Rooney, T.P., 2006. On defining and quantifying biotic homogenization. Glob. Ecol. Biogeogr. 15, 113–120. https://doi.org/10.1111/j.1466-822X.2006.00214.x.
Palmeggiani, G., Lebrun, M., Simiele, M., Bourgerie, S., Morabito, D., 2021. Effect of biochar application depth on a former mine technosol: impact on metal(loid)s and Alnus growth. Environments 8, 120. https://doi.org/10.3390/environments8110120.
Papatheodorou, E.M., Monokrousos, N., Angelina, E., Stamou, G.P., 2021. Robustness of rhizosphere microbial communities of *L. sativa* originated from soils of different legacy after inoculation with plant growth promoting rhizobacteria. Appl. Soil Ecol. 167, 104028. https://doi.org/10.1016/j.apsoil.2021.104028.
Pavlopoulos, G.A., Secrier, M., Moschopoulos, C.N., Soldatos, T.G., Kossida, S., Aerts, J., Schneider, R., Bagos, P.G., 2011. Using graph theory to analyze biological networks. BioData Mining 4, 10. https://doi.org/10.1186/1756-0381-4-10.
Pokharel, P., Ma, Z., Chang, S.X., 2020. Biochar increases soil microbial biomass with changes in extra- and intracellular enzyme activities: a global meta-analysis. Biochar 2, 65–79. https://doi.org/10.1007/s42773-020-00039-1.
Quilliam, R.S., Glanville, H.C., Wade, S.C., Jones, D.L., 2013. Life in the 'charosphere' – does biochar in agricultural soil provide a significant habitat for microorganisms? Soil Biol. Biochem. 65, 287–293. https://doi.org/10.1016/j.soilbio.2013.06.004.
Rawstern, A.H., Hernandez, D.J., Afkhami, M.E., 2025. Central taxa are keystone microbes during early succession. Ecol. Lett. 28, e70031. https://doi.org/10.1111/ele.70031.
Ren, Y., Ge, W., Dong, C., Wang, H., Zhao, S., Li, C., Xu, J., Liang, Z., Han, Y., 2023. Specialist species of fungi and bacteria are more important than the intermediate and generalist species in near-urban agricultural soils. Appl. Soil Ecol. 188, 104894. https://doi.org/10.1016/j.apsoil.2023.104894.
Rizwan, A., Zia-ur-Rehman, M., Rizwan, M., Usman, M., Anayatullah, S., Areej, Alharby, H.F., Bamagoos, A.A., Alharbi, B.M., Ali, S., 2023. Effects of silicon nanoparticles and conventional Si amendments on growth and nutrient accumulation by maize (*Zea mays* L.) grown in saline-sodic soil. Environ. Res. 227, 115740. https://doi.org/10.1016/j.envres.2023.115740.
Rong, X., Wu, N., Yin, B., Zhou, X., Zhu, B., Li, Y., Aanderud, Z.T., Zhang, Y., 2024. Degradation of wild fruit forests created less diverse and diffuse bacterial communities decreased bacterial diversity, enhanced fungal pathogens and altered

microbial assembly in the Tianshan Mountain, China. Plant Soil 501, 23–38. https://doi.org/10.1007/s11104-024-06545-6.
Rosseel, Y., 2012. lavaan: an R package for structural equation modeling. J. Stat. Softw. 48 (2), 1–36. https://doi.org/10.18637/jss.v048.i02.
Roughgarden, J., 1972. Evolution of niche width. Am. Nat. 106, 683–718. https://doi.org/10.1086/282807.
Segarra, S., Ribeiro, A., 2016. Stability and continuity of centrality measures in weighted graphs. IEEE Trans. Signal Process. 64, 543–555. https://doi.org/10.1109/TSP.2015.2486740.
Shi, G., Hou, R., Fu, Q., Li, T., Chen, Q., 2024. Effects of biochar and compost on microbial community assembly and metabolic processes in glyphosate, imidacloprid and pyraclostrobin polluted soil under freezethaw cycles. J. Hazard. Mater. 471, 134397. https://doi.org/10.1016/j.jhazmat.2024.134397.
Sloan, W.T., Lunn, M., Woodcock, S., Head, I.M., Nee, S., Curtis, T.P., 2006. Quantifying the roles of immigration and chance in shaping prokaryote community structure. Environ. Microbiol. 8, 732–740. https://doi.org/10.1111/j.1462-2920.2005.00956.x.
Spearman, C., 1904. The proof and measurement of association between two things. Am. J. Psychol. 15 (1), 72–101. https://doi.org/10.2307/1412159.
Stamou, G.P., Monokrousos, N., Papapostolou, A., Papatheodorou, E.M., 2023. Recurring heavy rainfall resulting in degraded-upgraded phases in soil microbial networks that are reflected in soil functioning. Soil Ecol. Lett. 5, 220161. https://doi.org/10.1007/s42832-022-0161-3.
Stegen, J.C., Lin, X., Fredrickson, J.K., Konopka, A.E., 2015. Estimating and mapping ecological processes influencing microbial community assembly. Front. Microbiol. 6. https://doi.org/10.3389/fmicb.2015.00370.
Sultana, U., Vanamala, P., Gul, M.Z., 2022. Cyanobacteria for bioremediation of contaminated soil. In: Malik, J.A. (Ed.), Microbial and Biotechnological Interventions in Bioremediation and Phytoremediation. Springer International Publishing, Cham, pp. 203–220. https://doi.org/10.1007/978-3-031-08830-8_9.
Sun, J., Zhou, H., Cheng, H., Chen, Z., Wang, Y., 2024a. Distinct strategies of the habitat generalists and specialists in the Arctic sediments: assembly processes, co-occurrence patterns, and environmental implications. Mar. Pollut. Bull. 205, 116603. https://doi.org/10.1016/j.marpolbul.2024.116603.
Sun, R., You, X., Cheng, Y., Gan, D., Suo, F., Wang, B., Li, Y., 2022. Response of microbial compositions and interactions to biochar amendment in the peanut-planted soil of the Yellow River Delta, China. Front. Environ. Sci. 10. https://doi.org/10.3389/fenvs.2022.924358.
Thion, C., Cébron, A., Beguiristain, T., Leyval, C., 2012. Long-term in situ dynamics of the fungal communities in a multi-contaminated soil are mainly driven by plants. FEMS Microbiol. Ecol. 82, 169–181. https://doi.org/10.1111/j.1574-6941.2012.01414.x.
Tipton, L., Müller, C.L., Kurtz, Z.D., Huang, L., Kleerup, E., Morris, A., Bonneau, R., Ghedin, E., 2018. Fungi stabilize connectivity in the lung and skin microbial ecosystems. Microbiome 6, 12. https://doi.org/10.1186/s40168-017-0393-0.
Tucker, C.M., Shoemaker, L.G., Davies, K.F., Nemergut, D.R., Melbourne, B.A., 2016. Differentiating between niche and neutral assembly in metacommunities using null models of β-diversity. Oikos 125, 778–789. https://doi.org/10.1111/oik.02803.
Valiente-Banuet, A., Aizen, M.A., Alcántara, J.M., Arroyo, J., Cocucci, A., Galetti, M., García, M.B., García, D., Gómez, J.M., Jordano, P., Medel, R., Navarro, L., Obeso, J. R., Oviedo, R., Ramírez, N., Rey, P.J., Traveset, A., Verdú, M., Zamora, R., 2019. Beyond Species Loss: extinction of Interactions in a Changing World.
Van Valen, L., 1965. Morphological variation and width of ecological niche. Am. Nat. 99 (908), 377–390. https://doi.org/10.1086/282379.
Vázquez, D.P., Simberloff, D., 2002. Ecological specialization and susceptibility to disturbance: conjectures and refutations. Am. Nat. 159, 606–623. https://doi.org/10.1086/339991.
Viotti, C., Albrecht, K., Amaducci, S., Bardos, P., Bertheau, C., Blaudez, D., Bothe, L., Cazaux, D., Ferrarini, A., Govilas, J., Gusovius, H.-J., Jeannin, T., Lühr, C., Müssig, J., Pilla, M., Placet, V., Puschenreiter, M., Tognacchini, A., Yung, L., Chalot, M., 2022. Nettle, a long-known fiber plant with new perspectives. Materials 15 (12), 4288. https://doi.org/10.3390/ma15124288.
Wang, C., Kuzyakov, Y., 2024. Mechanisms and implications of bacterial–fungal competition for soil resources. ISME J. 18, wrae073. https://doi.org/10.1093/ismejo/wrae073.
Wang, Z., Deng, G., Hu, C., Hou, X., Zhang, X., Fan, Z., Zhao, Y., Peng, M., 2025. Microbial diversity and community assembly in heavy metal-contaminated soils: insights from selenium-impacted mining areas. Front. Microbiol. 16, 1561678. https://doi.org/10.3389/fmicb.2025.1561678.
Wu, C., Ren, H., Liu, Z., Lu, H., Huang, Y., Jian, S., Hui, D., Liu, H., Zhu, C., Zhang, S., He, X., 2024. Spatial heterogeneity of resource availability drives soil bacterial community assembly along the sandy coast of Southern China. Global Ecol. Conserv. 54, e03171. https://doi.org/10.1016/j.gecco.2024.e03171.
Wu, X., Yang, J., Ruan, H., Wang, S., Yang, Y., Naeem, I., Wang, L., Liu, L., Wang, D., 2021. The diversity and co-occurrence network of soil bacterial and fungal communities and their implications for a new indicator of grassland degradation. Ecol. Indic. 129, 107989. https://doi.org/10.1016/j.ecolind.2021.107989.
Xiang, L., Harindintwali, J.D., Wang, F., Redmile-Gordon, M., Chang, S.X., Fu, Y., He, C., Muhoza, B., Brahushi, F., Bolan, N., Jiang, X., Ok, Y.S., Rinklebe, J., Schaeffer, A., Zhu, Y., Tiedje, J.M., Xing, B., 2022. Integrating biochar, bacteria, and plants for sustainable remediation of soils contaminated with organic pollutants. Environ. Sci. Technol. 56, 16546–16566. https://doi.org/10.1021/acs.est.2c02976.
Xing, W., Gai, X., Ju, F., Chen, G., 2023. Microbial communities in tree root-compartment niches under Cd and Zn pollution: structure, assembly process and co-occurrence relationship. Sci. Total Environ. 860, 160273. https://doi.org/10.1016/j.scitotenv.2022.160273.
Xiong, X., Wang, W., Xing, Y., Chen, H., Luo, X., Chen, W., Huang, Q., 2022. Niche overlap is a predictor of the interspecies correlations detected by microbial network analysis in soil micro-aggregates. J. Soils Sediments 22, 1521–1529. https://doi.org/10.1007/s11368-022-03165-4.
Xu, Q., Vandenkoornhuyse, P., Li, L., Guo, J., Zhu, C., Guo, S., Ling, N., Shen, Q., 2022. Microbial generalists and specialists differently contribute to the community diversity in farmland soils. J. Adv. Res. 40, 17–27. https://doi.org/10.1016/j.jare.2021.12.003.
Xu, W., Xu, H., Delgado-Baquerizo, M., Gundale, M.J., Zou, X., Ruan, H., 2023. Global *meta*-analysis reveals positive effects of biochar on soil microbial diversity. Geoderma 436, 116528. https://doi.org/10.1016/j.geoderma.2023.116528.
Yaashikaa, P.R., Kumar, P.S., Varjani, S., Saravanan, A., 2020. A critical review on the biochar production techniques, characterization, stability and applications for circular bioeconomy. Biotechnol. Rep. 28, e00570. https://doi.org/10.1016/j.btre.2020.e00570.
Yachi, S., Loreau, M., 1999. Biodiversity and ecosystem productivity in a fluctuating environment: the insurance hypothesis. Proc. Natl. Acad. Sci. 96, 1463–1468. https://doi.org/10.1073/pnas.96.4.1463.
Yates, C.F., Trexler, R.V., Bonet, I., King, W.L., Hockett, K.L., Bell, T.H., 2022. Rapid niche shifts in bacteria following conditioning in novel soil environments. Funct. Ecol. 36, 3085–3095. https://doi.org/10.1111/1365-2435.14180.
Yuan, M.M., Guo, X., Wu, Linwei, Zhang, Y., Xiao, N., Ning, D., Shi, Z., Zhou, X., Wu, Liyou, Yang, Y., Tiedje, J.M., Zhou, J., 2021. Climate warming enhances microbial network complexity and stability. Nat. Clim. Chang. 11, 343–348. https://doi.org/10.1038/s41558-021-00989-9.
Zhalnina, K., Louie, K.B., Hao, Z., Mansoori, N., da Rocha, U.N., Shi, S., Cho, H., Karaoz, U., Loqué, D., Bowen, B.P., Firestone, M.K., Northen, T.R., Brodie, E.L., 2018. Dynamic root exudate chemistry and microbial substrate preferences drive patterns in rhizosphere microbial community assembly. Nat. Microbiol. 3, 470–480. https://doi.org/10.1038/s41564-018-0129-3.
Zhang, J., 2016. spaa: Species Association Analysis. R Package Version 0.2.2. Available at: https://CRAN.R-project.org/package=spaa.
Zhang, M., Zhang, T., Zhou, L., Lou, W., Zeng, W., Liu, T., Yin, H., Liu, H., Liu, X., Mathivanan, K., Praburaman, L., Meng, D., 2022. Soil microbial community assembly model in response to heavy metal pollution. Environ. Res. 213, 113576. https://doi.org/10.1016/j.envres.2022.113576.
Zhao, J., Qiu, Yingbo, Yi, F., Li, J., Wang, X., Fu, Q., Fu, X., Yao, Z., Dai, Z., Qiu, Yunpeng, Chen, H., 2024. Biochar dose-dependent impacts on soil bacterial and fungal diversity across the globe. Sci. Total Environ. 930, 172509. https://doi.org/10.1016/j.scitotenv.2024.172509.
Zhong, Y., Sorensen, P.O., Zhu, G., Jia, X., Liu, J., Shangguan, Z., Wang, R., Yan, W., 2022. Differential microbial assembly processes and co-occurrence networks in the soil-root continuum along an environmental gradient. Soil Ecol. Lett. 4, 168–179. https://doi.org/10.1002/imt2.18.
Zhou, J., Ning, D., 2017. Stochastic community assembly: does it matter in microbial ecology? Microbiol. Mol. Biol. Rev. 81 (4). https://doi.org/10.1128/mmbr.00002-17.
Zhou, H., Zhang, D., Wang, P., Liu, X., Cheng, K., Li, L., Zheng, J., Zhang, X., Zheng, J., Crowley, D., van Zwieten, L., Pan, G., 2017. Changes in microbial biomass and the metabolic quotient with biochar addition to agricultural soils: a meta-analysis. Agric. Ecosyst. Environ. 239, 80–89. https://doi.org/10.1016/j.agee.2017.01.006.
Zhu, N., Yu, Q., Song, L., Sheng, H., 2023. The inhibiting effects of high-dose biochar application on soil microbial metagenomics and rice (Oryza sativa L.) production. Int. J. Mol. Sci. 24, 15043. https://doi.org/10.3390/ijms242015043.
Zhu, Y., Ge, X., Wang, L., You, Y., Cheng, Y., Ma, J., Chen, F., 2022. Biochar rebuilds the network complexity of rare and abundant microbial taxa in reclaimed soil of mining areas to cooperatively avert cadmium stress. Front. Microbiol. 13. https://doi.org/10.3389/fmicb.2022.972300.
Zou, X., Jiang, X., Guan, J., Huang, S., Chen, C., Zhou, T., Kuang, C., Ye, J., Liu, T., Cheng, J., Chen, S., Yu, S., 2024. Both organic fertilizer and biochar applications enhanced soil nutrition but inhibited cyanobacterial community in paddy soils. Front. Environ. Sci. 12. https://doi.org/10.3389/fenvs.2024.1376147.